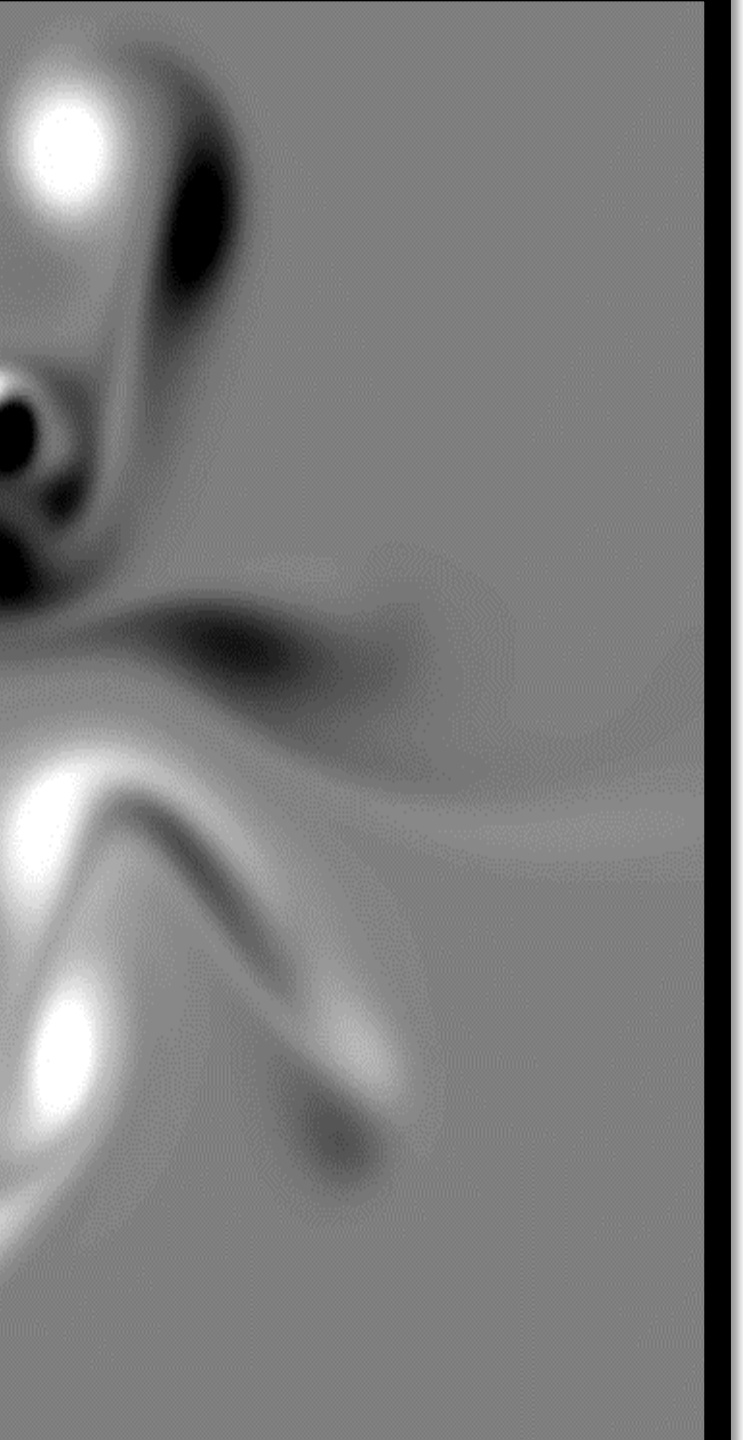

ReCoVor Seminar Series 102A

Immersed Boundary–Aware Physics-Informed Surrogates for Unsteady Moving-Body Flows

Capabilities, Insights, and Open Challenges

Rahul Sundar
PhD Scholar / Scientist (AI/ML)
Dept. of Aerospace Engineering, IIT Madras / Verisk, India
Email – rahulsundar@smail.iitm.ac.in

Dr. Didier Lucor
CNRS France, University of Paris - Saclay

Prof. Sunetra Sarkar
Dept. of Aerospace Engineering
IIT Madras

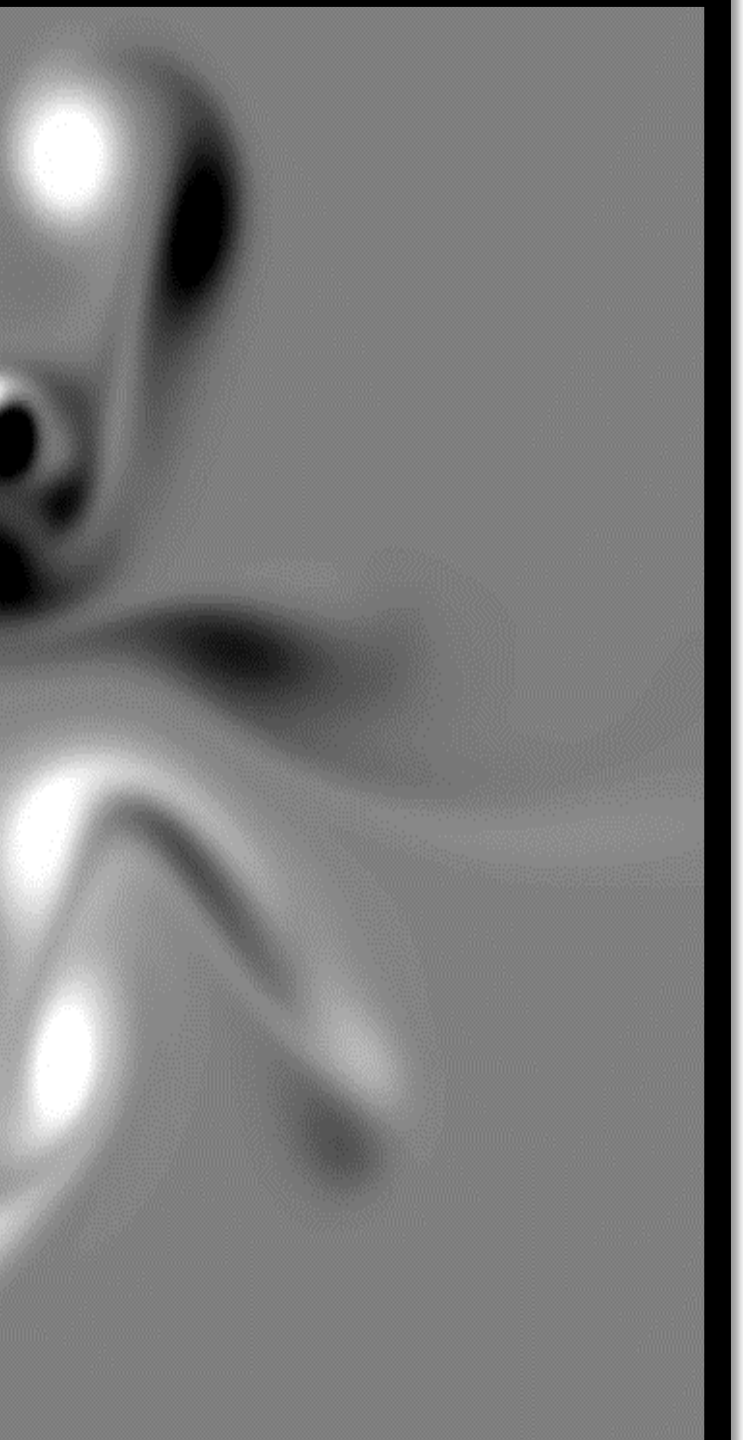

Outline

Key research question: **"Can we recover hidden flow physics from sparse data — even when boundaries move?"**

- Challenges in surrogate modelling for moving boundary flows: **Data & Modeling complexities**
- **Our wish list & desired applications**
- Immersed boundary aware framework: **The three key ideas**
- **Salient results**
- **Key Takeaways**

Challenges in surrogate modelling for moving boundary flows

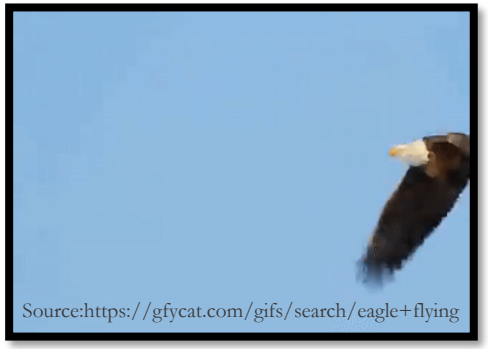

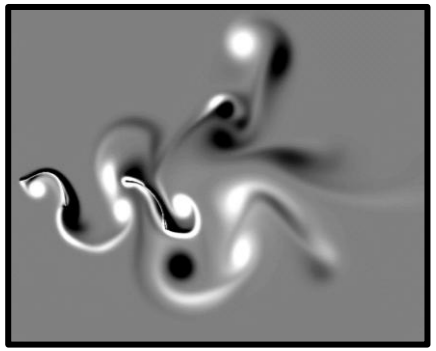

Source:https://www.lalchhoteshah.com/

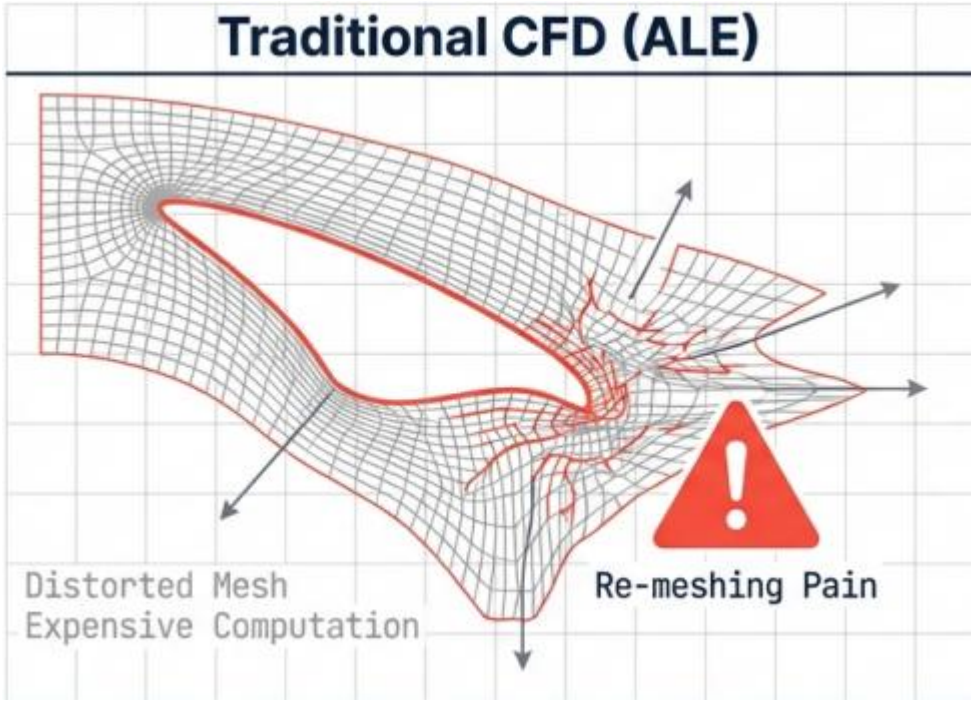

→ **Strongly vortex dominated** – strong flow-field gradients – around the moving body

→ Simulations – body conformal (ALE)/**non-conformal (IBM) mesh approaches – preferred**

→ Parametric exploration, **data storage, real time query – expensive →Surrogates!**

Challenges in surrogate modelling for moving boundary flows

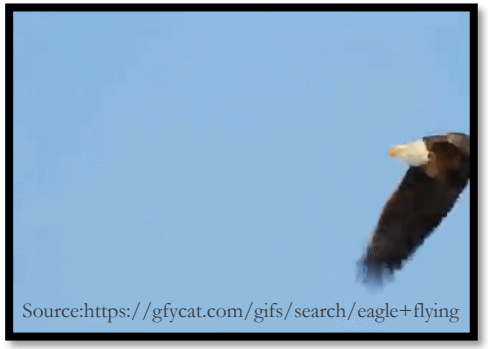

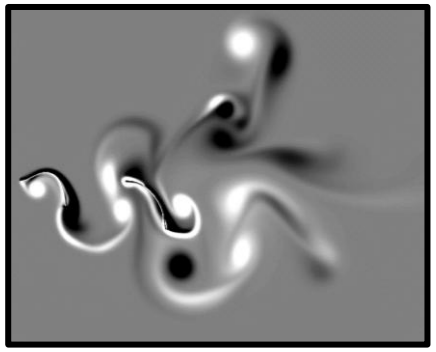

Source:https://www.lalchhoteshah.com/

Immersed boundary methods

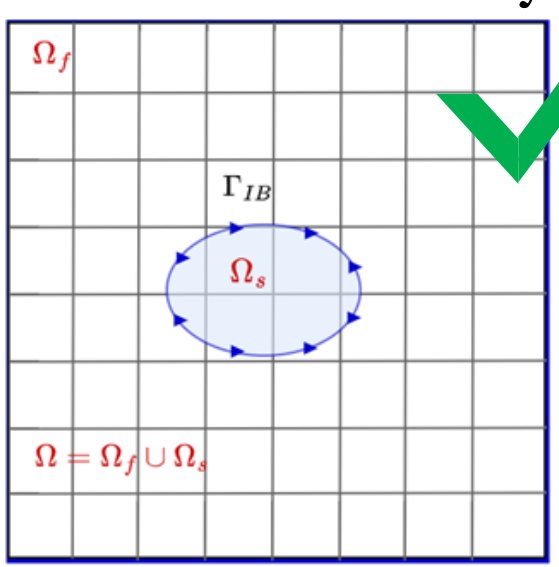

No mesh-motion and re-meshing,

Fixed Eulerian frame of reference

→ **Strongly vortex dominated** – strong flow-field gradients – around the moving body

→ Simulations – body conformal (ALE)/**non-conformal (IBM) mesh approaches – preferred**

→ Parametric exploration, **data storage, real time query – expensive →Surrogates!**

Challenges in surrogate modelling: **Data and Modeling Complexities**

Types of **temporal domain complexities** in the context of Unsteady flow datasets

1) Sparsity, 2) Long time domain, and 3) Aperiodicity

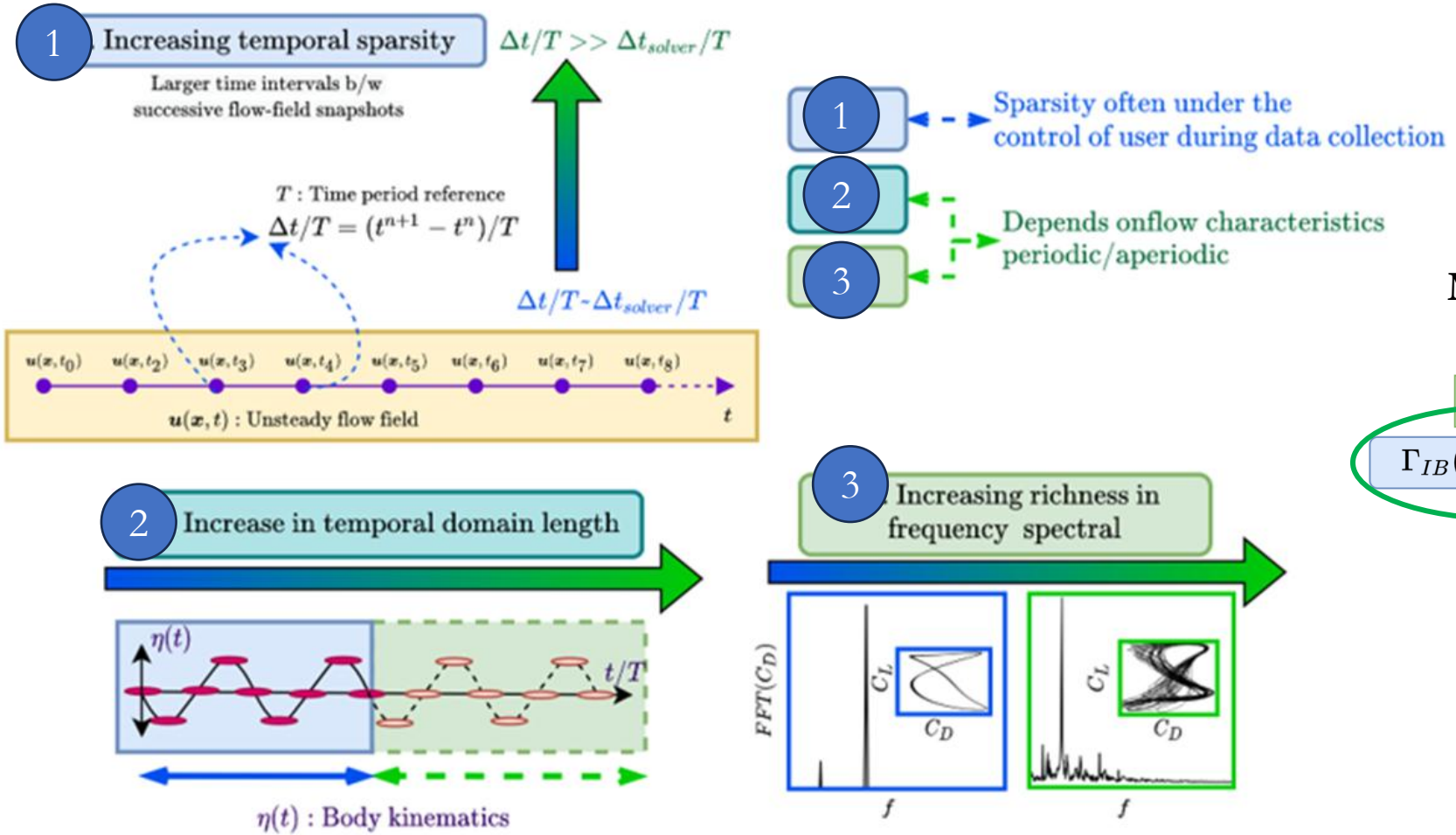

1 — Sparsity often under the control of user during data collection

2 — Depends onflow characteristics periodic/aperiodic

3 — Depends onflow characteristics periodic/aperiodic

Moving body configuration known vs. unknown

Scenarios

$\Gamma_{IB}(t)$ **Known**

$\Gamma_{IB}(t)$ **Unknown**

Challenges for surrogate modeling: **Data & Modeling complexities**

Challenges posed for data-driven surrogate modelling using IBM data:

→ IBM obtained solutions – fictitious flow field Ω_s (solid region) → varying in time → Moving discontinuity

→ **Enforcing no-slip BC** on the solid boundary:

- **The IBM solution** - Disjoint representation of fluid **(Eulerian grid)** and Solid boundary **(Lagrangian Markers)**
- **Body forcing term (f)** in momentum conservation equation

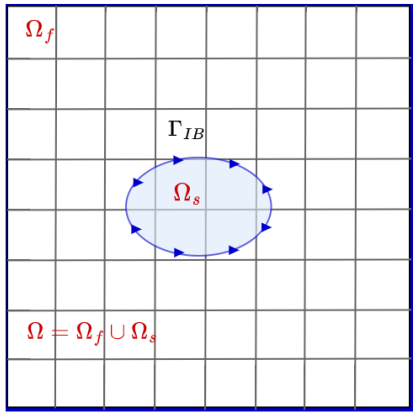

$\Gamma_{IB}(t)$ – Moving boundary
Ω_s, Ω_f – Solid & Fluid regions

Discrete forcing IBM (Incompressible flow)

[Kim *et al.* (2001), Majumdar *et al.* (2020)]

$$\frac{\partial \boldsymbol{u}}{\partial t} + \nabla.(\boldsymbol{uu}) = -\nabla p + \frac{1}{Re}\nabla^2 \boldsymbol{u} + \boldsymbol{f}$$

$$\nabla.\boldsymbol{u} - q = 0.$$

Our wish list

Based on the challenges and the attractive features of IBM, our requirements for an ideal framework are

1 **Grid agnosticity allowing any arbitrary domain & grid**

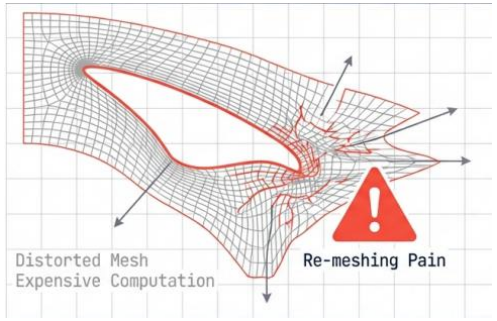

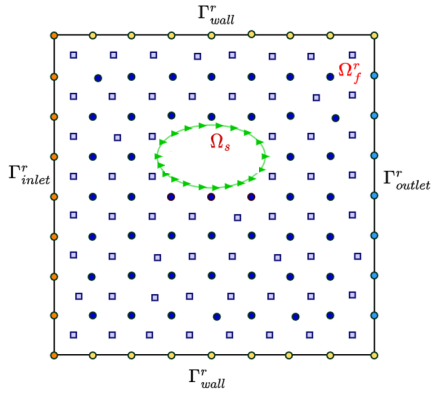

2 **Eulerian fixed frame of reference**

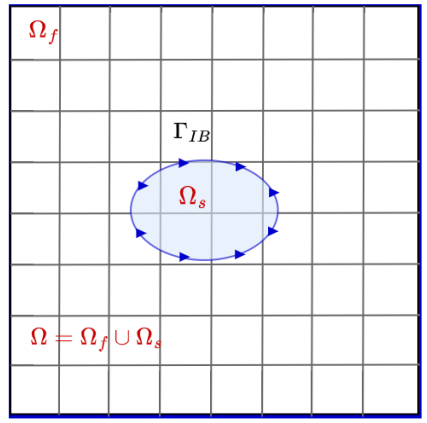

3 **Flexibility to handle both scenarios under spatio-temporal sparsity**

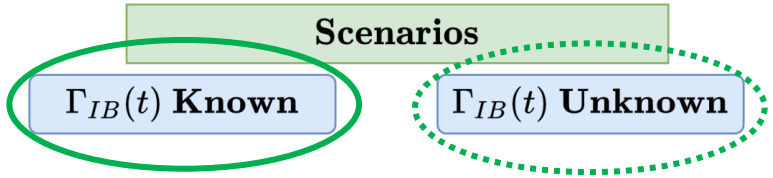

4 **Data efficiency**

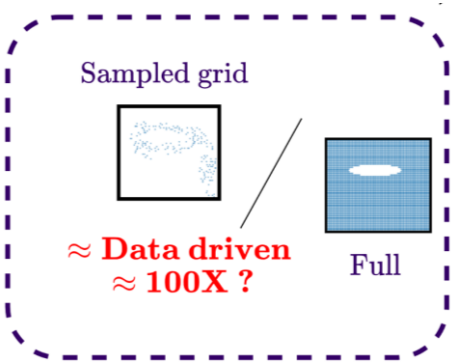

Desired Applications

1 **Non-intrusive hidden pressure recovery**

– **Instantaneous pressure fields –** desirable to understand sources driving aero-/hydrodynamic loads:
– **Simulations:** Some **IBM variants** – velocity alone needed for **load estimation – pressure data not stored** [Majumdar *et al.* (2020)]
– **Experiments:** – PIV Measurements of velocity [Dabiri *et al.* (2014)]

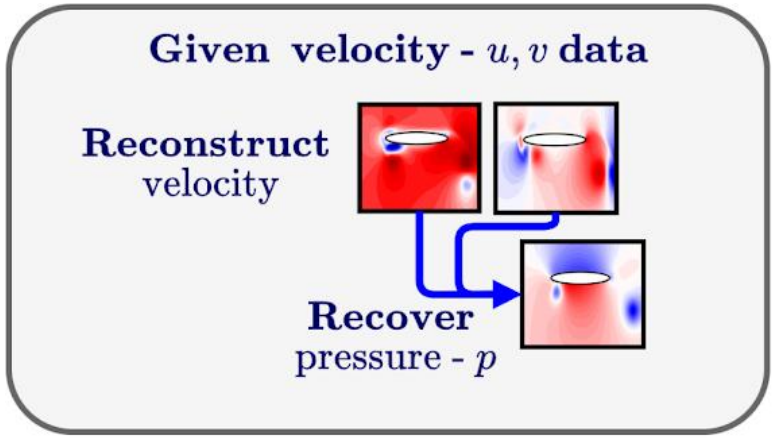

2 **Hidden boundary estimation** *(high complexity)*

Pressure recovery and moving body configuration estimation when body shape, position, and velocity are not known apriori

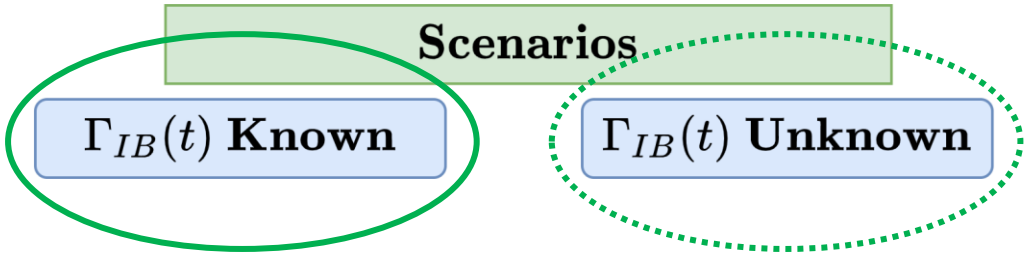

Potential of Physics informed neural networks

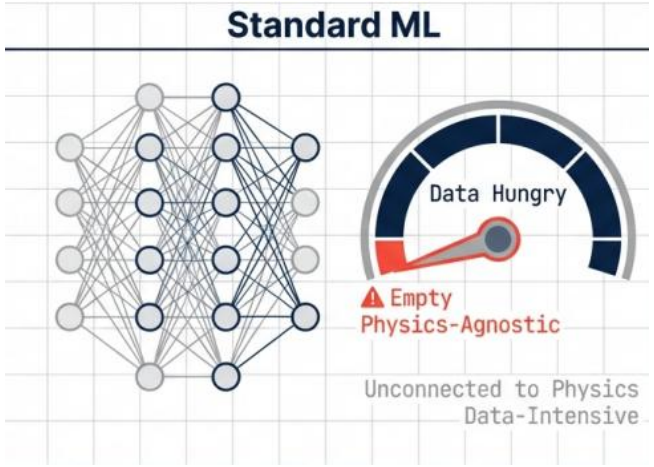

Physics informed neural networks (*Raissi et al. (2019), JCP***)**

1. **Physics-informed** loss + Data-driven loss
2. Can handle any **arbitrary domain / grid –** pointwise inputs!
3. **Flexible** to implement for **forward/inverse problems (Hidden variable recovery, hidden boundary estimation, etc.)**

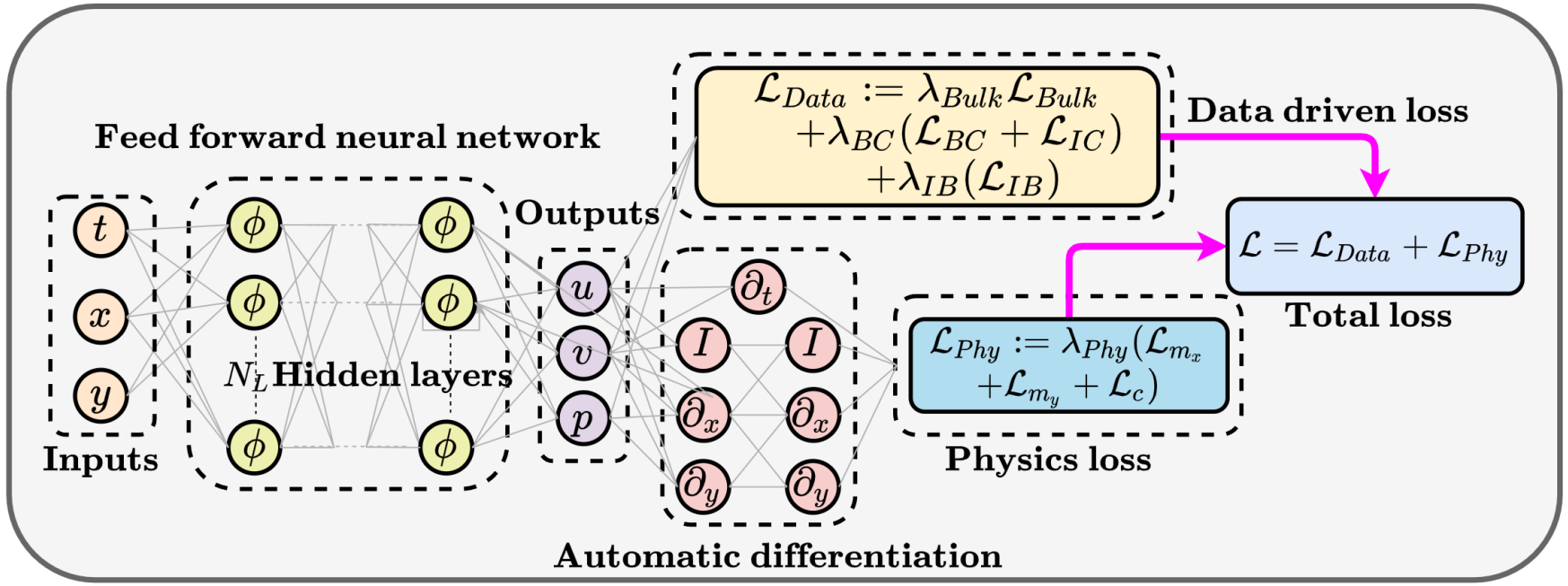

Immersed Boundary Aware (IBA) Framework

based on Physics Informed Neural Networks

IBA Framework – Dual PINN Formulations

Moving Boundary (MB) enabled PINNs (NS and IBM formulations)

MB-PINN (*Standard N-S GEqns.*)

MB-IBM-PINN (*IBM formulation GEqns.*)

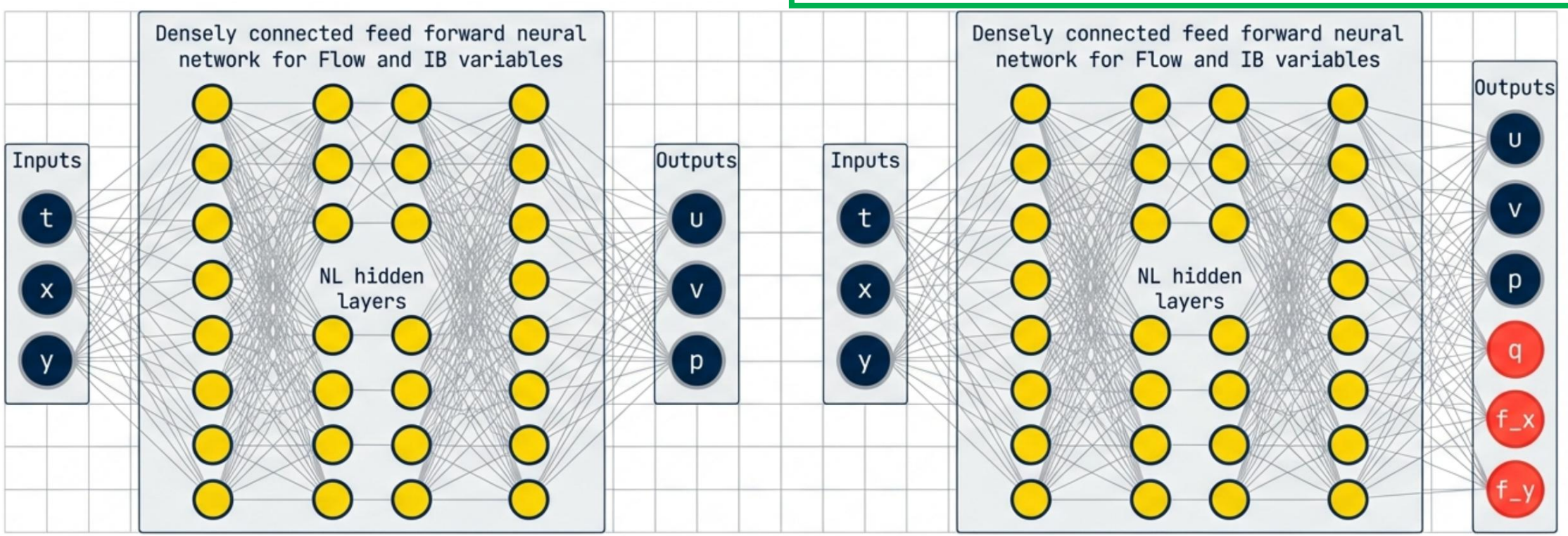

$$\mathcal{L} := \mathcal{L}_{Phy} + \mathcal{L}_{Data}$$

$$\mathcal{L}_{Phy} = \lambda_{fluid}\left(\mathcal{L}_{m_x} + \mathcal{L}_{m_y} + \mathcal{L}_c\right)^{\Omega_f} + \lambda_{solid}\left(\mathcal{L}_{m_x} + \mathcal{L}_{m_y} + \mathcal{L}_c\right)^{\Omega_s} \quad (1)$$

$$\mathcal{L}_{Data} = \lambda_{Bulk}\mathcal{L}_{Bulk} + \lambda_{inlet}\mathcal{L}_{inlet} + \lambda_{IB}\mathcal{L}_{IB} + \lambda_{IBvar}\mathcal{L}_{IBvar}$$

Plunging foil problem setup

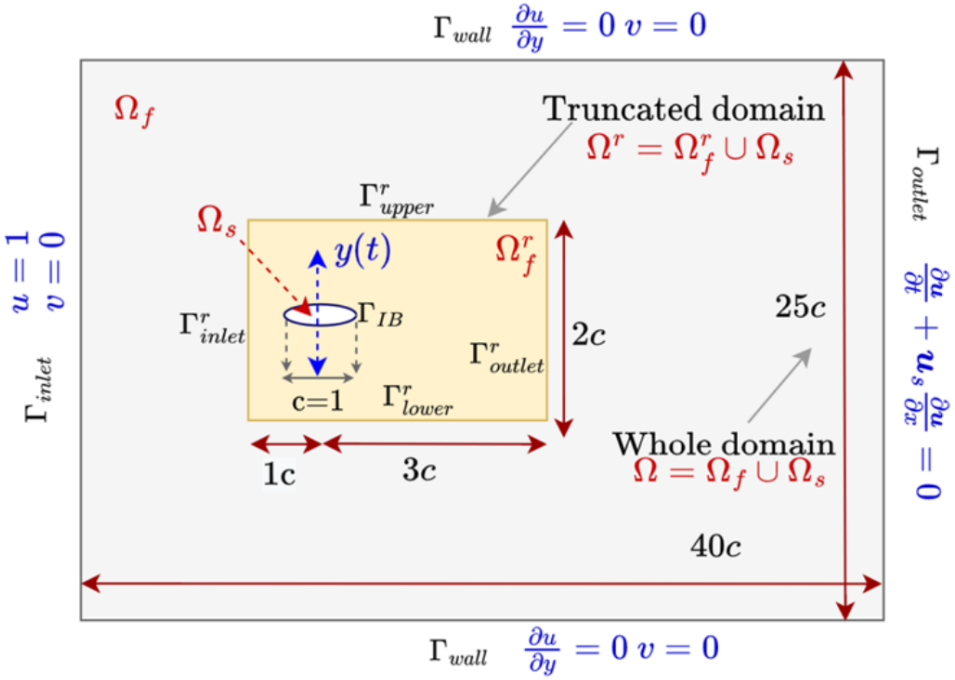

$$y(t) = h_a \cos(2\pi f_h t + \phi)$$
$$\dot{y}(t) = -2\pi f_h h_a \sin(2\pi f_h t + \phi)$$

h_a :Plunging Amplitude
ϕ :Phase
f_h :Pluning frequency
c : foil chord length

Ω_f, Ω_f^2 :Whole and truncated fluid domains
Ω_s :Solid domain
$\Gamma_{\#}$: **inlet, walls, outlet** boundaries of whole domain Ω
Γ^r_* : **inlet, outlet, lower & upper** boundaries of truncated domain Ω^r

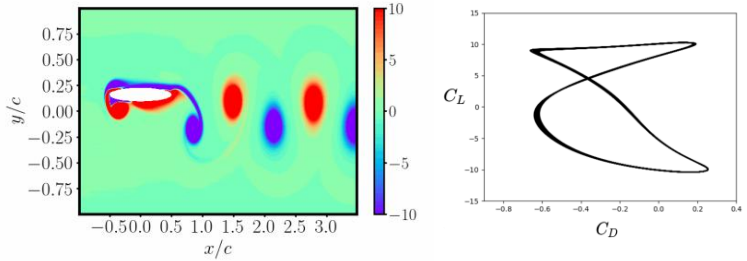

Case 1: Periodic

$Re = 500, h_a = 0.16, f_h = 1, c = 1, U_\infty = 1$

[validated with Khalid et al. (2015)]

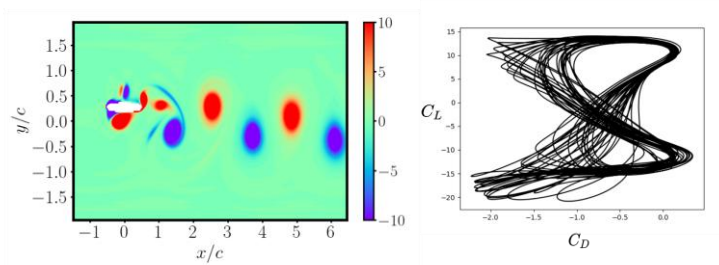

Case 2: Quasi-Periodic

$Re = 300, h_a = 0.4125, f_h = 4, c = 1, U_\infty = 1$

[validated with Majumdar et al. (2019)]

Plunging foil problem setup

Computational domain: $(x, y) \in [-1.5, 3.5] \times [-1.0, 1.0]$

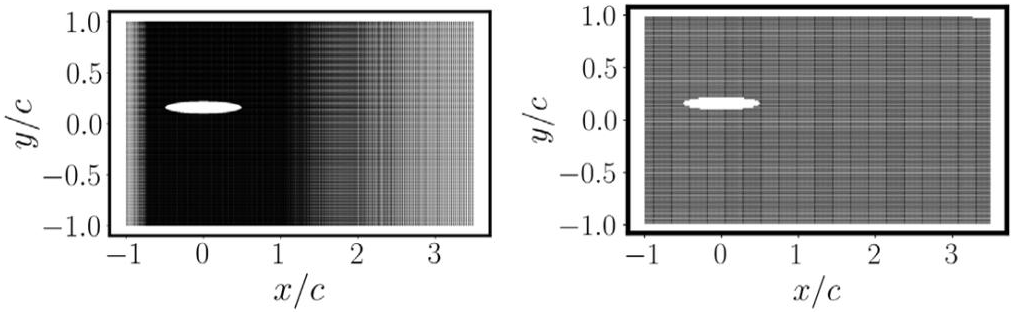

(a) IBM grid
$Nx * Ny = 325500, \Delta x = \Delta y = 0.004$

(b) Coarsened grid
$Nx * Ny = 30000, \Delta x = \Delta y = 0.016$

Interpolate IBM grid data onto a relatively coarse grid (~10% the size)

Computational domain: $(x, y) \in [-1.5c, 6.5c] \times [-2.0c, 2.0c]$

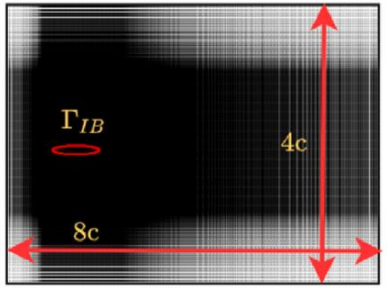

(a) High resolution IBM grid
$Nx * Ny = 443592, , \Delta x = \Delta y = 0.004$

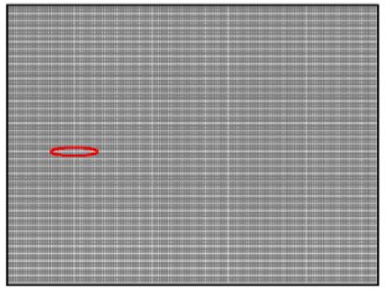

(b) Coarsened grid
$Nx * Ny = 45000, \Delta x = \Delta y = 0.026$

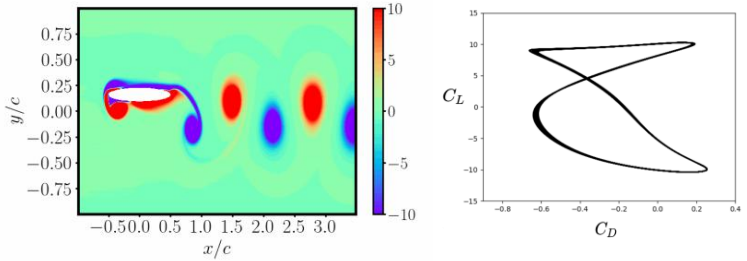

Case 1: Periodic

$Re = 500, h_a = 0.16, f_h = 1, c = 1, U_\infty = 1$

[validated with Khalid et al. (2015)]

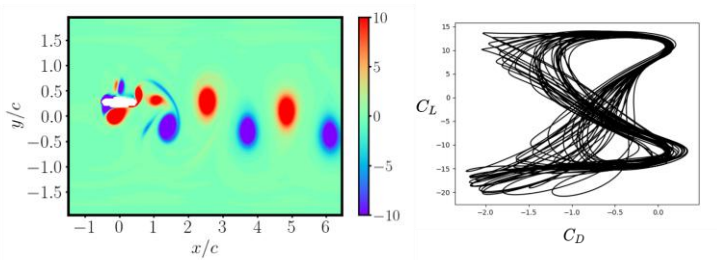

Case 2: Quasi-Periodic

$Re = 300, h_a = 0.4125, f_h = 4, c = 1, U_\infty = 1$

[validated with Majumdar et al. (2019)]

Key contribution #1 – Physics-Aware training design
Multipart physics loss weighting

Multipart physics loss weighting-

$$\mathcal{L}_{Phy} = \lambda_{fluid}\mathcal{L}_{Phy}^{fluid} + \lambda_{solid}\mathcal{L}_{Phy}^{solid}$$

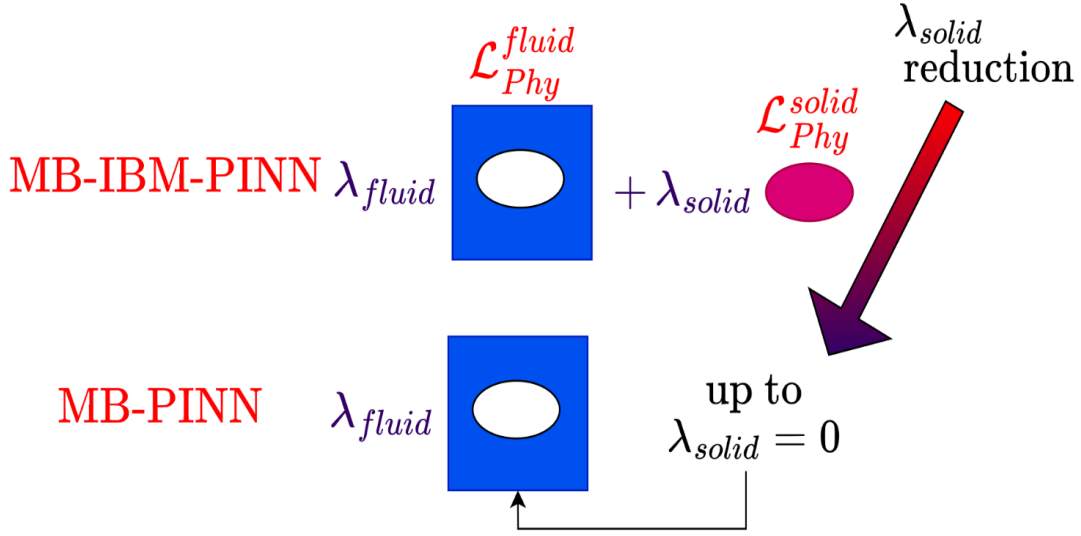

1. Explain conditions under which **MB-PINN and MB-IBM-PINN are equivalent**
2. Explain role of **Solid domain** in model performance of MB-IBM-PINN
3. Explain scenarios where **MB-PINN** or **MB-IBM-PINN** are applicable

Key contribution #1 – Physics-Aware training design
Multi-part loss weighting & hidden pressure recovery

1 **MB-IBM-PINN equivalent to MB-PINN when $\lambda_{solid} = 0$**

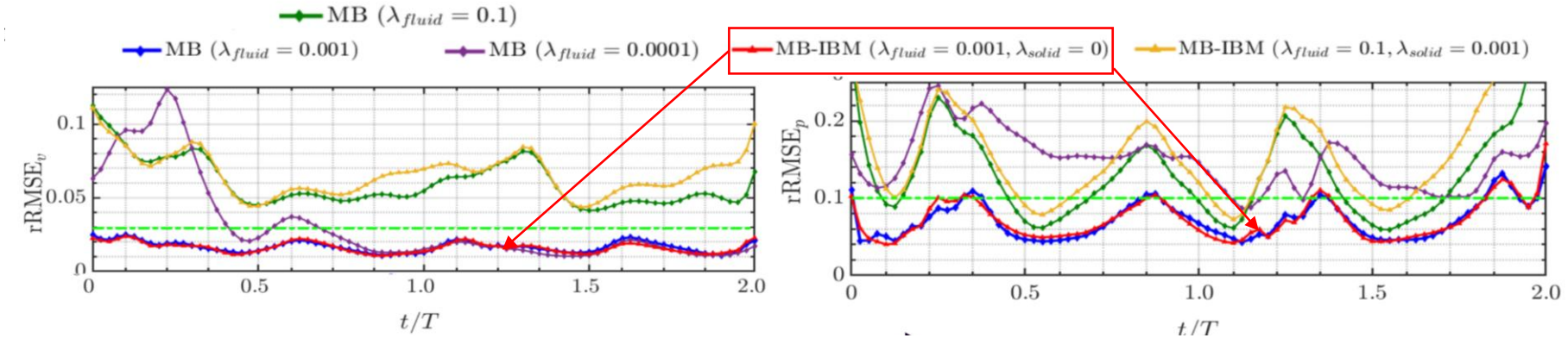

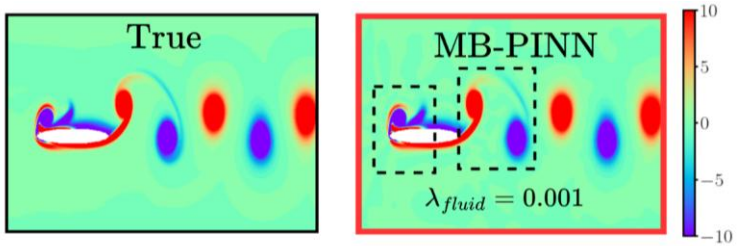

2 **If solid body position and velocity known L_{Phy}^{solid} → Ω_s can be discarded!**

At optimal $\lambda_{fluid} = 0.001$,

$\lambda_{solid} = 0$

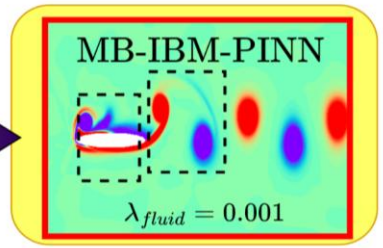

3 But what if body configuration is not known? – **MB-IBM-PINN has potential**

Hidden Boundary estimation

Pressure recovery when body shape, position, and velocity are not known apriori

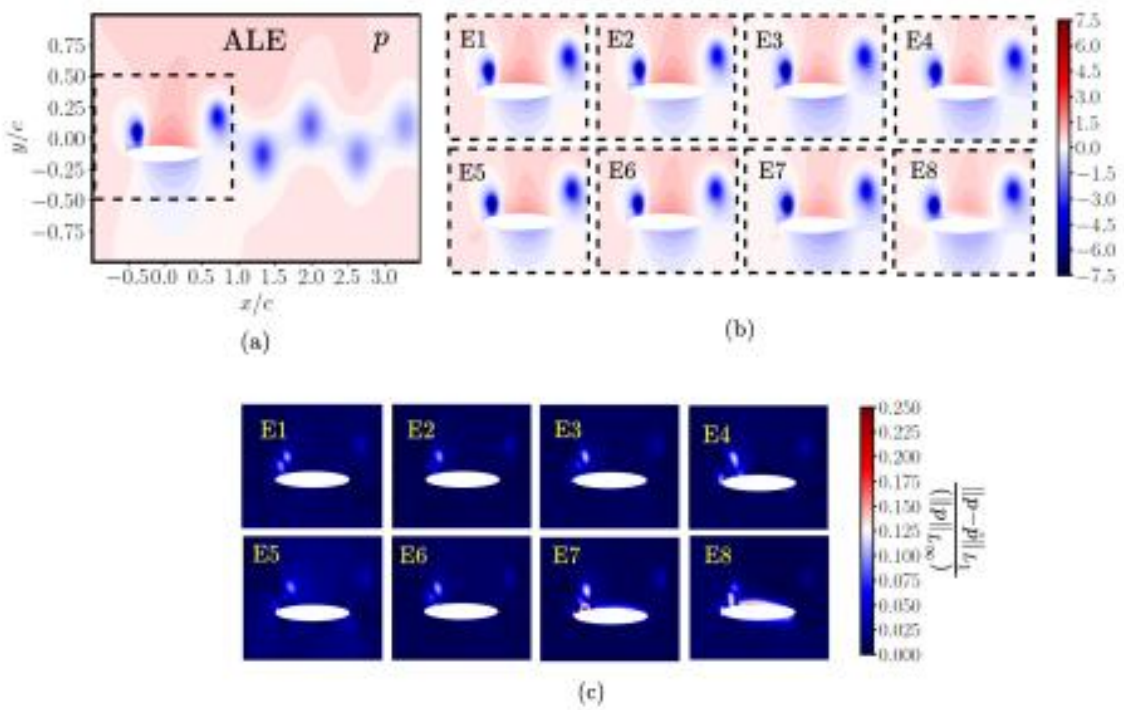

Figure 8: Comparison of (a) true ALE pressure with the (b) predictions obtained from optimal MB-PINN (with and without $\mathcal{L}_{IB}$ constraint) and MB-IBM-PINN(without $\mathcal{L}_{IB}$ constraint) models and (c) corresponding maximum value normalised pointwise absolute error contours. The rectangular boxes in (b) and (c) representing the near-field region in (a) marked by E1 $\lambda_{fluid} = 0.001, \gamma = 1$ - taken from the manuscript), E2-E4 (MB-PINN - $\lambda = 0.001, \gamma = 0$ with fluid data points sampled 2, 5 and 10 cells away from the solid boundary, respectively), E5 (MB-IBM-PINN - $\lambda = 0.01, \gamma = 0, \xi = 1$(no VF)), and E6-E8 (MB-IBM-PINN - $\lambda = 0.001, \gamma = 0, \xi = 1$ (VF) with fluid data points sampled 2, 5 and 10 cells away from the solid boundary, respectively).

Given velocity data away from the moving boundary:

Steps involved:

1. **Train MB-IBM-PINNs** to obtain velocity, recover pressure and IBM auxillary variables $\boldsymbol{f}$ and q.

Hidden Boundary estimation

Preliminary extension to body shape estimation using MB-IBM-PINN

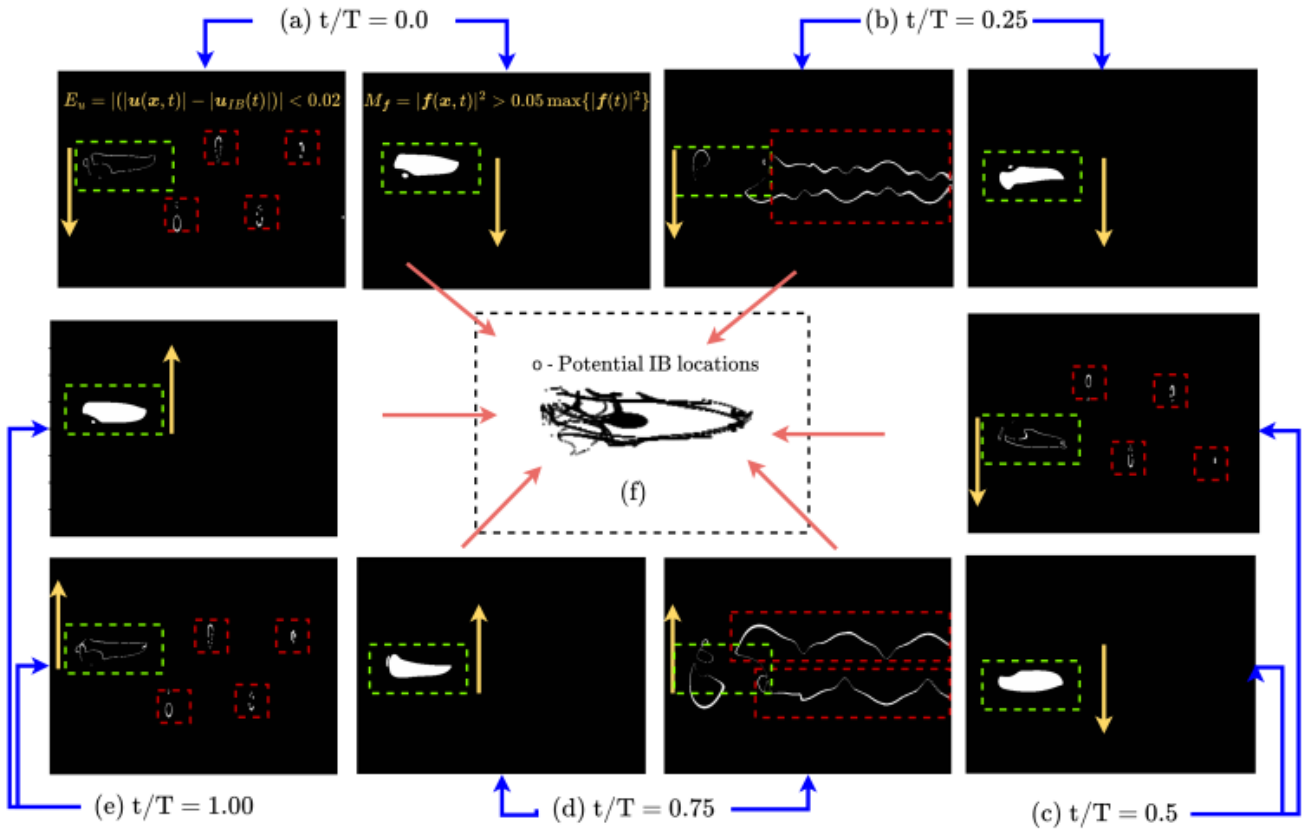

Figure 15: Detailed representation of (a)-(e) extracting the potential IB marker locations by combining the body velocity magnitude based edge extraction ($E_{|\boldsymbol{u}_{IB}|}$) with the masks $M_{\boldsymbol{f}}(t)$ at different time instants. The extracted potential IB marker locations are depicted in (f).

Given velocity data away from the moving boundary:

Steps involved:

1. **Train MB-IBM-PINNs** to obtain velocity, pressure and IBM auxillary variables $\boldsymbol{f}$ and q.
2. **Extract edges** based on velocity fields
3. **Extract masks** using $\boldsymbol{f}$
4. **Combine masks and edges** to obtain a cluster of potential IB marker locations.

Hidden Boundary estimation

Preliminary extension to body shape estimation using MB-IBM-PINN

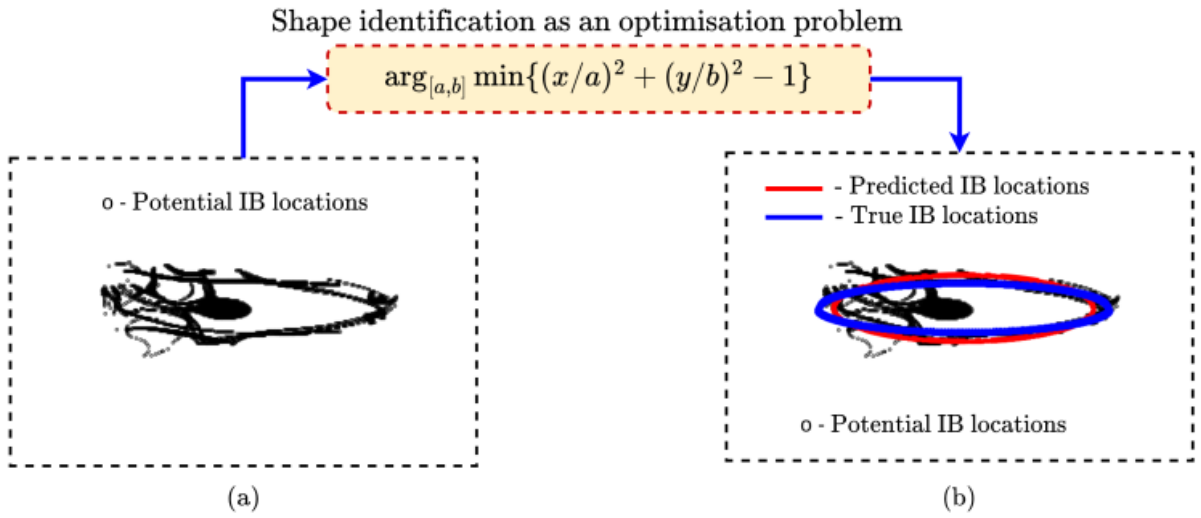

Figure 16: Shape estimation as an optimisation problem. (a) The extracted potential IB marker locations and (b) overlay of the true and predicted IB.

Given velocity data away from the moving boundary:

Steps involved:

1. **Train MB-IBM-PINNs** to obtain velocity, pressure and IBM auxillary variables $\boldsymbol{f}$ and q.
2. **Extract edges** based on velocity fields
3. **Extract masks** using $\boldsymbol{f}$
4. **Combine masks and edges** to obtain a cluster of potential IB marker locations.
5. **Assume a shape prior (ellipse)** and determine the shape parameters.

Key contribution #2 – Physics-Aware training design

Vorticity cut off sampling

Vorticity cut off selection

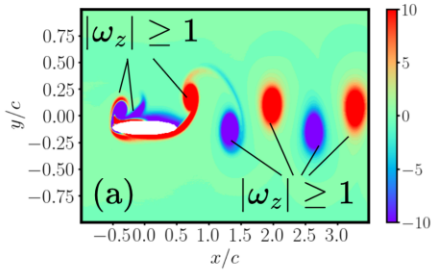

Snapwise relative RMSE for pressure p and velocity components v

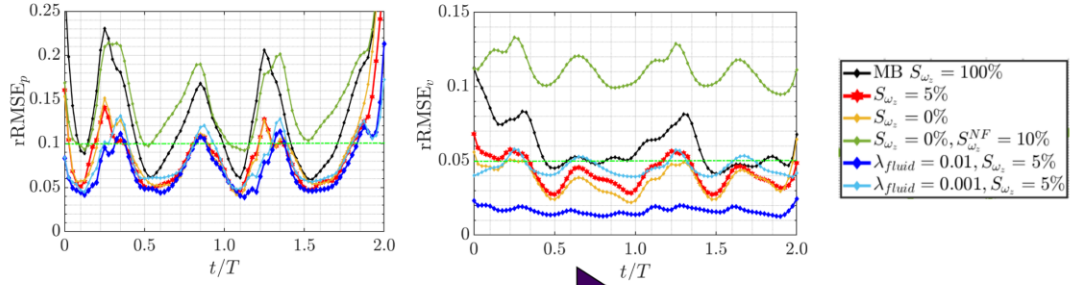

Vorticity cut-off based far field sampling ratio

$$S_{\omega_z} = 100 \times \frac{N^{sample}_{|\omega_z|<1}}{N_{|\omega_z|<1}}$$

Effect of S_{ω_z} reduction: Increasing data efficiency

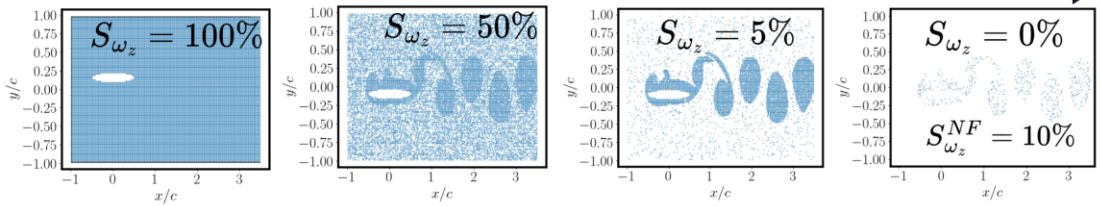

Near field sampling ratio

$$S^{NF}_{\omega_z} = 100 \times \frac{N^{sample}_{|\omega_z|\geq 1}}{N_{|\omega_z|\geq 1}}$$

Effect of S_{ω_z} reduction: Improved reconstruction of primary and seconday vortex structures

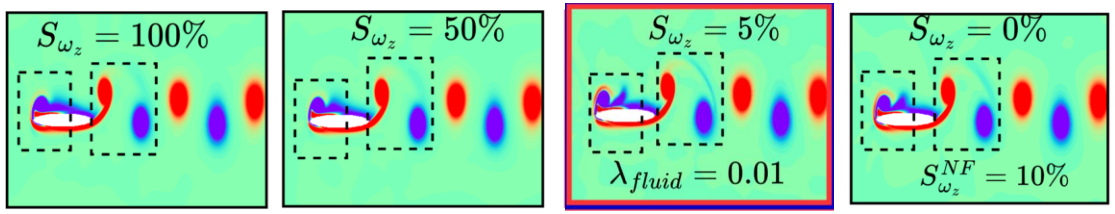

Optimal: $\lambda_{fluid} = 0.01$ *and* $S_{\omega_z} = 5\%$

→ ~ **1%** of the grid points in **Ref-IBM** grid.

→ 100 × **savings on memory**

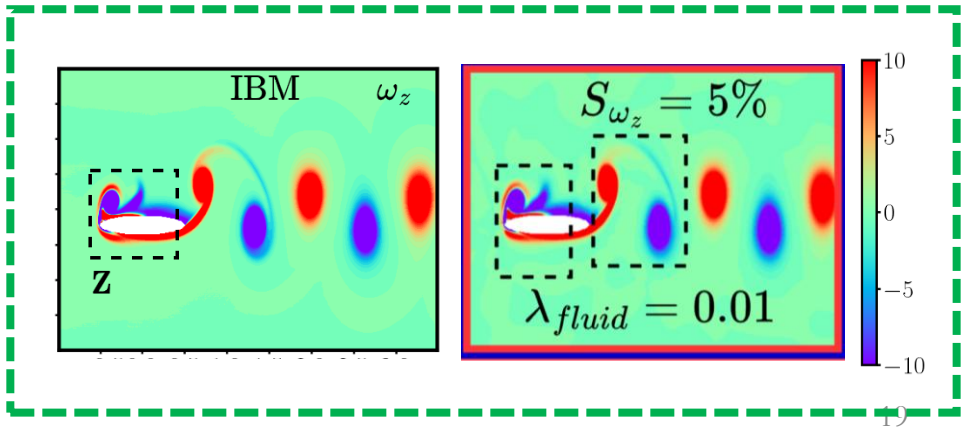

Key contribution #2 – Physics-Aware training design
Preferential spatio-temporal sampling

Computational domain: $(x, y) \in [-1.5c, 6.5c] \times [-2.0c, 2.0c]$

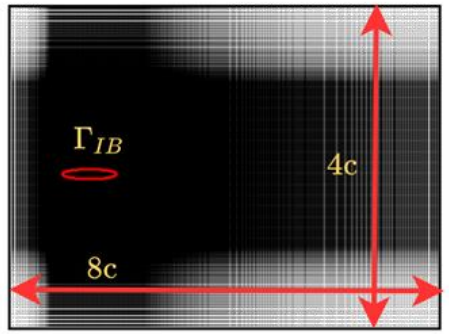

(a) High resolution IBM grid
$Nx * Ny = 443592, , \Delta x = \Delta y = 0.004$

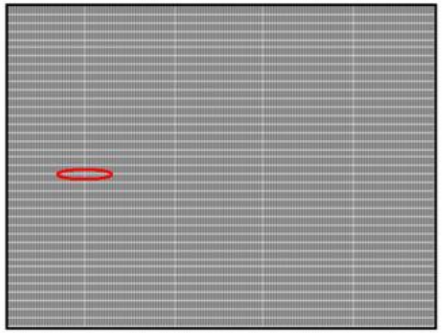

(b) Coarsened grid
$Nx * Ny = 45000, \Delta x = \Delta y = 0.026$

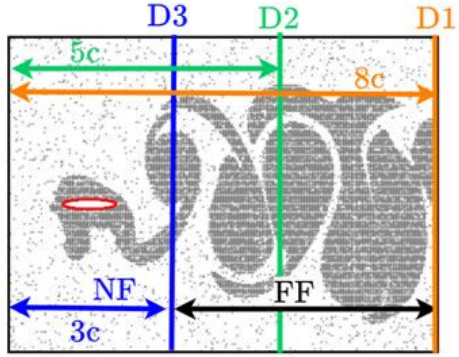

(c)Vorticity cutoff based under sampled grid
$Nx * Ny = 15610, |\omega_z^*| = 0.1$

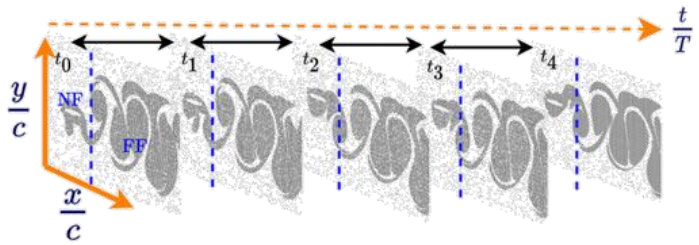

$\Delta t_{NF}/T = \Delta t_{FF}/T = (t_{i+1} - t_i) = 0.125$

(d) Vorticity cutoff based sampling

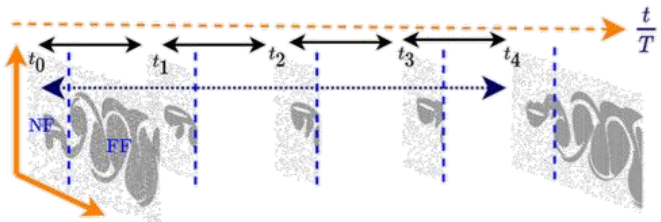

$\Delta t_{NF}/T = (t_{i+1} - t_i) = 0.125$
$\Delta t_{FF}/T = 0.5$

(e) Preferential spatio-temporal sampling

Key contribution #3 – Temporal learning
Time marching vs time domain decomposition, and transfer learning

Single network
Fixed temporal complexity

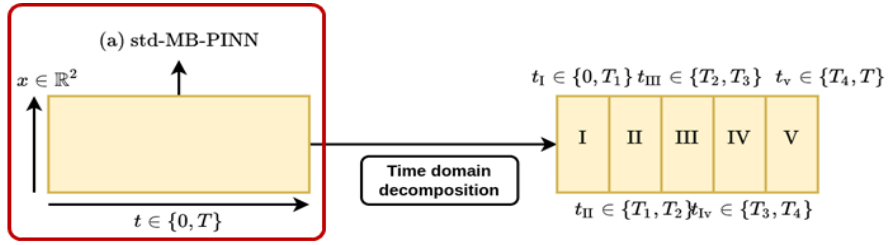

Class I: Single Network
Gradual increase in temporal complexity

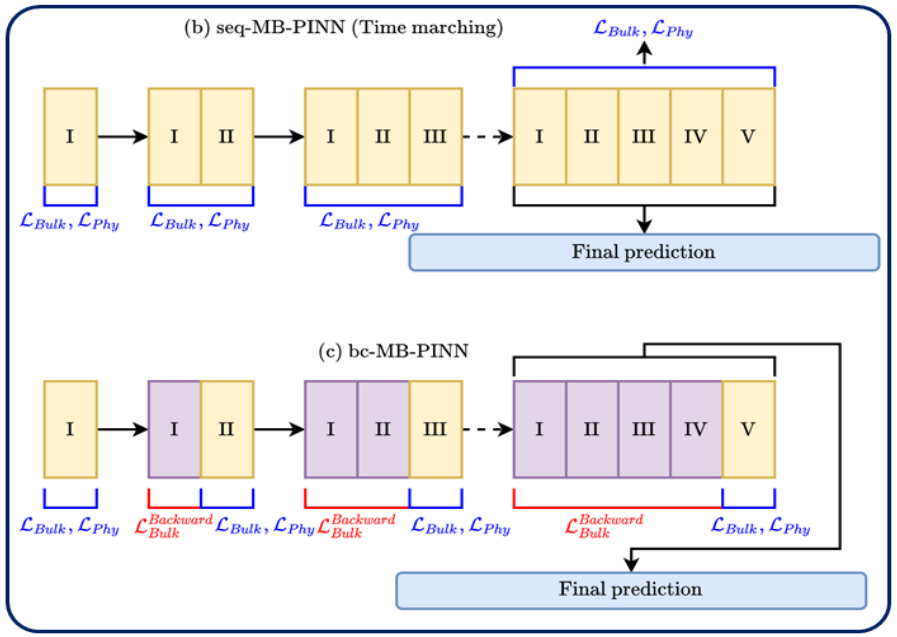

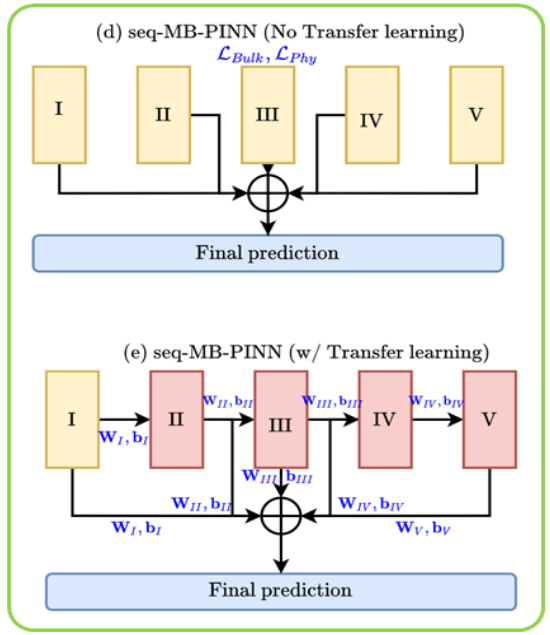

Class II: Multiple small networks
Reduced temporal complexity

Hyper parameters:
Layers $(l = 5, 10)$, Neurons $(n = 100, 225)$, Subdomains $N_d = 5$ over 10 cycles,
ADAM optimiser | N_{iter} = **5e05** iterations | 3 training cycles – [1e-03, 5e-04, 1e-04] | Mini batch – 1.5e03

Krishnapriyan et al. ANIPS (2021), Mattey et al. CMAE (2022), Penwarden et al. JCP (2023)

Case studies and salient results

Periodic flow case study

Importance of having a physics loss under temporal sparsity

Temporal sampling intervals
$\frac{\Delta t}{T} = [0.2, 0.25, 0.3, 0.4, 0.5]$

MB-FNN :
Data driven, no physics loss.
Compared with MB-PINN

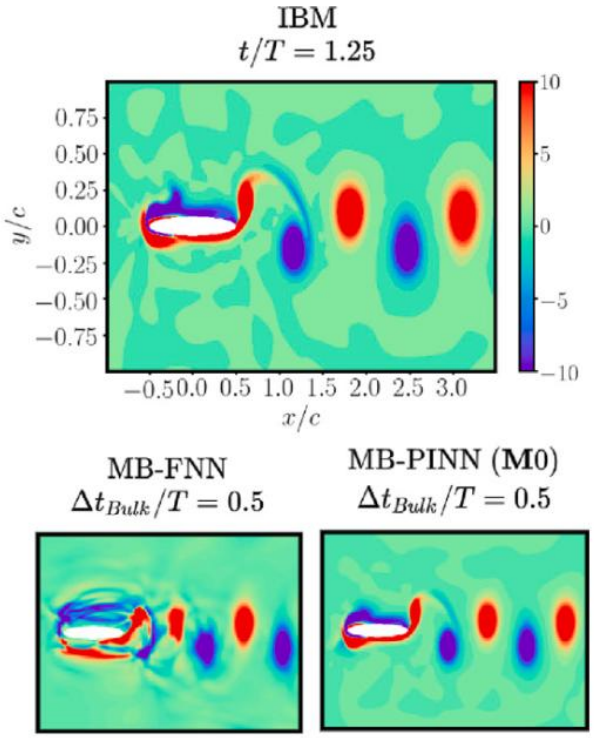

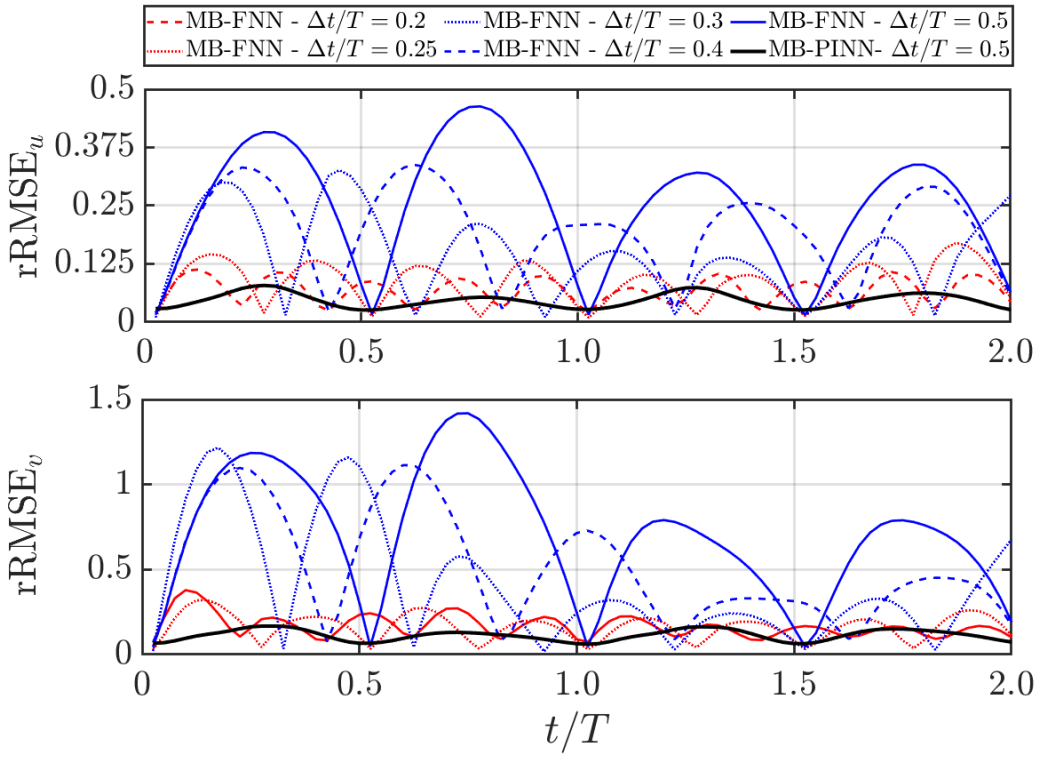

- **Physics loss is a good regulariser for temporally sparse datasets and can improve spatiotemporal interpolation**
- Hence **std-MB-PINN** better than purely data driven **(MB-FNN)** models in this case even under high sparsity.

Quasi-Periodic flow case study

Preferential sampling and relaxing of L_{IB} ($\lambda_{IB} = 1, 0.1, 0.01, 0.001$)

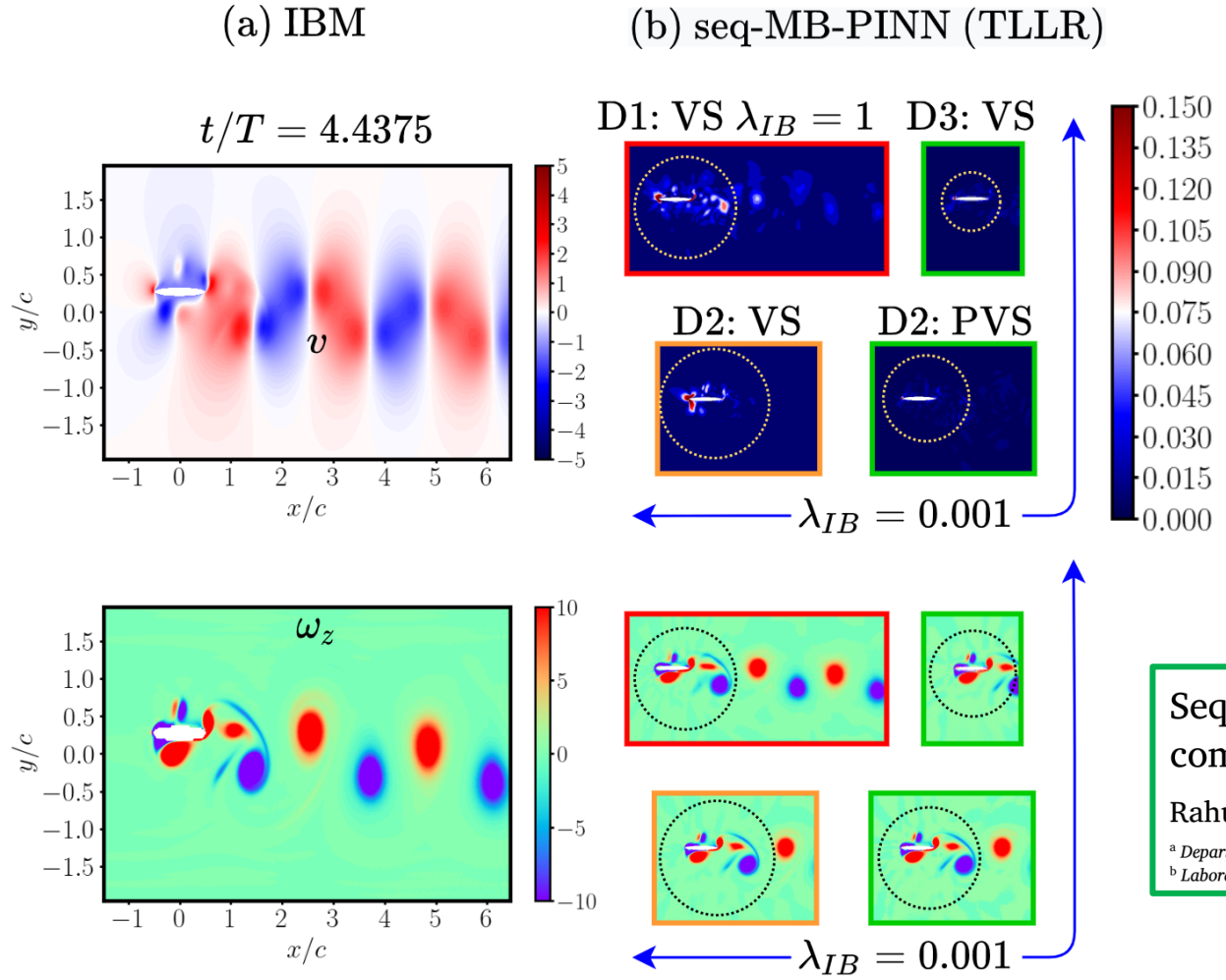

- Preferential sampling improves **nearfield velocity reconstruction**
- In fact, in scenarios where wake data is not available or not necessary for analysis, **near-field data alone suffices for velocity reconstruction.**

Sequential learning based PINNs to overcome temporal domain complexities in unsteady flow past flapping wings

Rahul Sundar [a], Didier Lucor [b], Sunetra Sarkar [a,*]

[a] *Department of Aerospace Engineering, Indian Institute of Technology Madras, Chennai, 600036, Tamil Nadu, India*
[b] *Laboratoire Interdisciplinaire des Sciences du Numérique LISN-CNRS, Orsay, 91403, France*

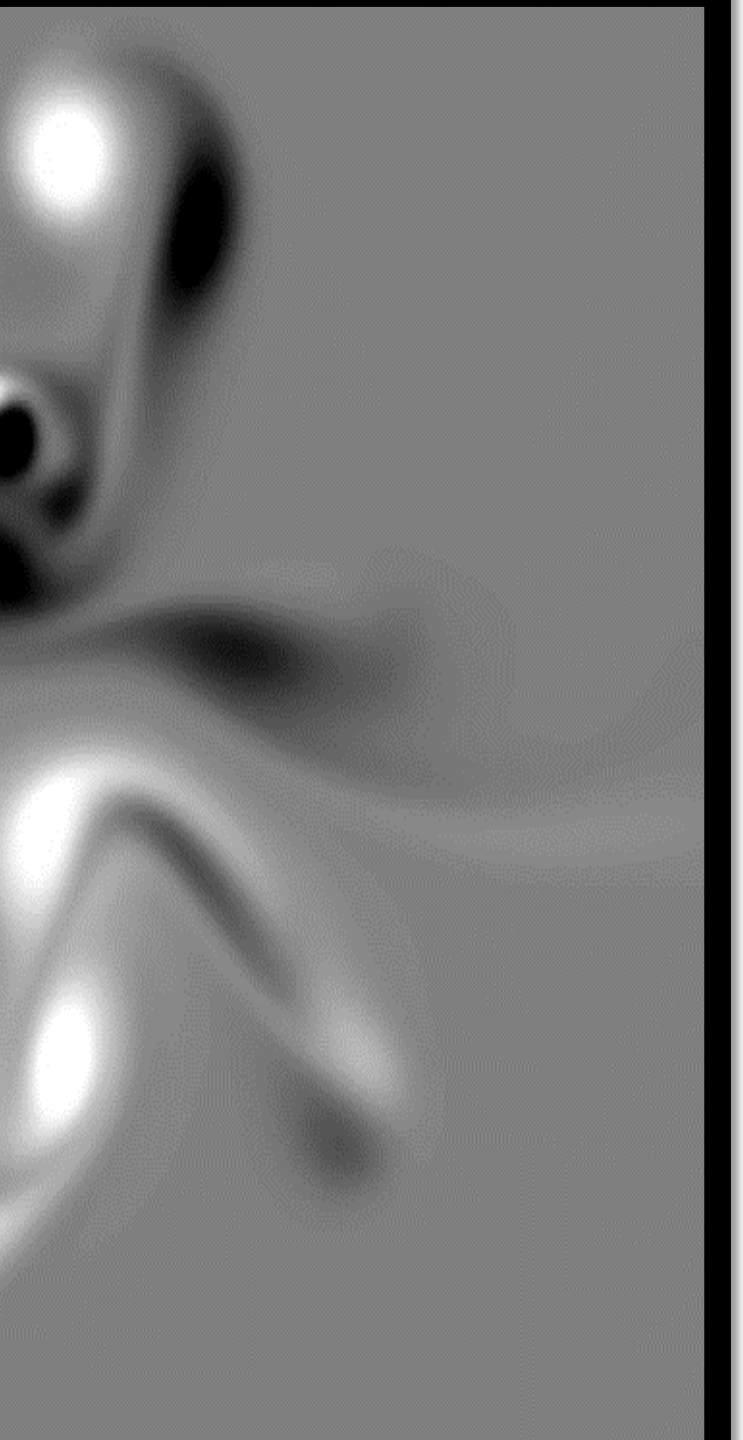

Key Takeaways

Yes, we recover hidden flow physics from sparse data — even when boundaries move – borrowing inspiration from IBM"

- Challenges in surrogate modelling for moving boundary flows: **Data & Modeling complexities**
- **Immersed boundary framework:** grid agnosticity, eulerian frame, flexibility to handle different data availability scenarios
- Immersed boundary aware framework: **The three key ideas**
  - Multipart loss weighting, physics-based sampling, sequential learning and transfer learning
- **Salient results:**
  - Hidden pressure recovery from just near-field data for Quasi-periodic flows
  - Hidden boundary estimation/approximation and simultaneous pressure recovery
- **Future directions/ open challenges:**
  - Multiple moving bodies, flexible deforming bodies
  - 3D flows and chaotic flows
  - Parametric operator based model
  - Single foundational model to handle forward/ inverse problems

Rahul Sundar

Bio-Mimetics & Dynamics

$\mathcal{L}\alpha\beta$

Thank you

Appendix

- IBM data reconstruction – An ML problem
- Overview of the IBA framework
- Detailed MB-PINN and MB-IBM-PINN architecture and formulation
- Training vs testing approach
- Additional results from periodic case study
- Quasi-periodic case study – additional results – Aerodynamic load reconstruction
- Present and other contemporary works
- Other ongoing works in the lab

IBM data reconstruction: **An ML problem**

Spatio-temporal velocity data obtained from IBM

$$X = [\boldsymbol{u}(\boldsymbol{x}, t_0), \boldsymbol{u}(\boldsymbol{x}, t_0), \boldsymbol{u}(\boldsymbol{x}, t_1), \cdots \boldsymbol{u}(\boldsymbol{x}, t_{N_t-1}), \boldsymbol{u}(\boldsymbol{x}, t_{N_t}))]_{2N_{\boldsymbol{x}} \times N_t}$$

Linear Mapping

Alternating Least Squares approximation (ALS)

$\hat{X} = AB$

$\hat{X} = U\Sigma V^T$

POD, DMD, SPOD

Least-squares optimal low-rank decomposition

$\arg\min_X \|X - \hat{X}\|_{L_2}^2$

Affine / conformal coordinate transformations to body attached reference frame

Eulerian reference frame

No closed form approximation!

~~$\hat{X} = U\Sigma V^T$~~

$\hat{X} = AB$

$\arg\min_{\hat{X}} \|\mathbf{M} \odot (X - \hat{X})\|_{L_2}^2$

Mask-weighted low-rank decomposition
(Balajewicz et al. (2014))

Autoregressive mapping

$\hat{X} = \Psi(\Phi(X))$

$\hat{X} = F(\boldsymbol{x}, t)$

Full-field / Point-wise mapping

$\hat{X} = F(\boldsymbol{x}, t)$

$\hat{X} = \Psi(\Phi(X))$

Non-linear mapping

M - Binary mask of fluid vs. moving solid region (ghost cells in IBM)

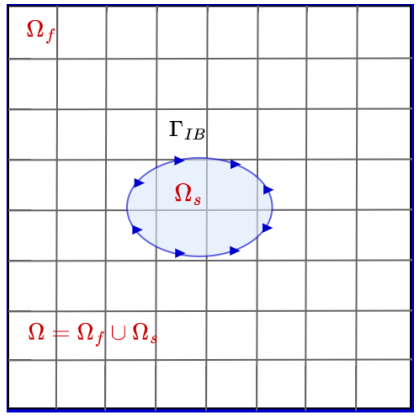

Discrete forcing IBM (Incompressible flow)

[Kim *et al.* (2001), Majumdar *et al.* (2020)]

$$\frac{\partial \boldsymbol{u}}{\partial t} + \nabla.(\boldsymbol{u}\boldsymbol{u}) = -\nabla p + \frac{1}{Re}\nabla^2 \boldsymbol{u} + \boldsymbol{f}$$

$$\nabla.\boldsymbol{u} - q = 0.$$

IBA framework overview

Physics-informed neural networks modelling for systems with moving immersed boundaries: Application to an unsteady flow past a plunging foil

Rahul Sundar [a], Dipanjan Majumdar [a], Didier Lucor [b], Sunetra Sarkar [a,*]

[a] Department of Aerospace Engineering, Indian Institute of Technology Madras, Chennai, 600036, Tamil Nadu, India
[b] Université Paris-Saclay, CNRS, Laboratoire Interdisciplinaire des Sciences du Numérique (LISN), Orsay, F91405, France

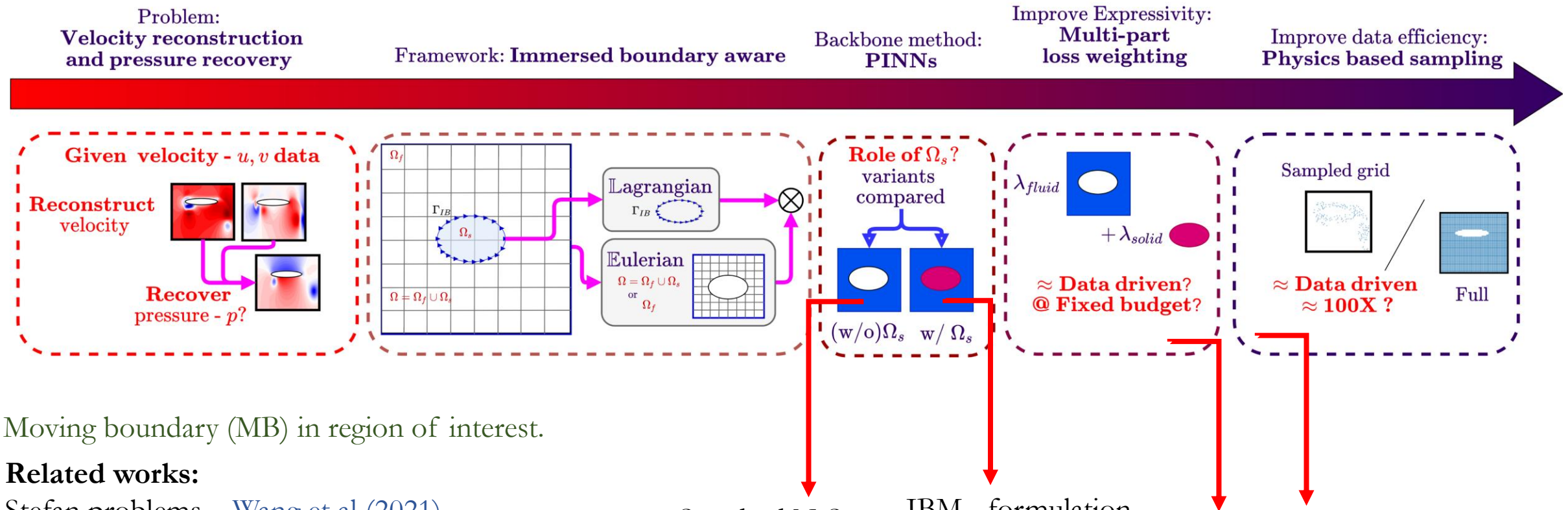

Moving boundary (MB) in region of interest.

Related works:

Stefan problems – Wang et al (2021)

Two-phase flows moving interface – Buhendwa et al. (2021)

Standard N-S MB-**PINN**

IBM - formulation MB-**IBM-PINN**

Loss weighting and sampling [Lucor et al (2022), Yang et al (2022), Gopakumar *et al.* (2022)]

Immersed boundary aware framework

Near field pressure recovery

Framework-Immersed boundary aware

PINN variants: MB-PINN/ MB-IBM-PINNs

Improve data efficiency- Physics based sampling

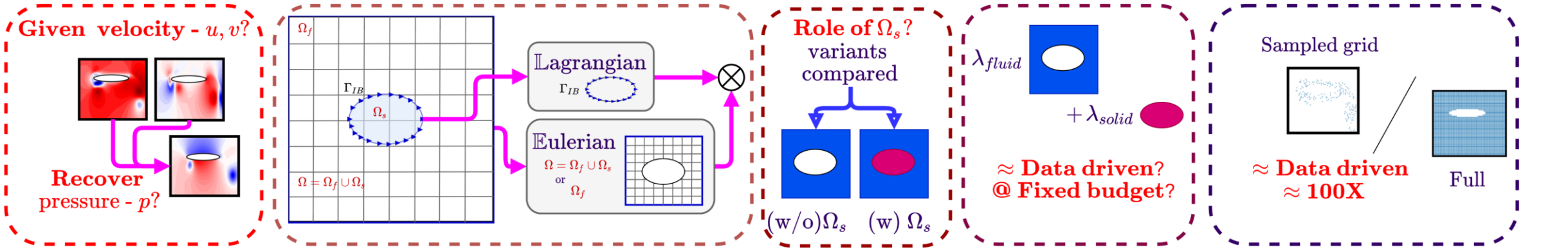

1. General framework!

2. Flexibly handled by PINNs!

3. Balanced contributions from data & physics with physics loss relaxation

4. Residual collocation points from moving solid region not necessary if Γ_{IB} position and velocity known *apriori*.

5. Physics based sampling - Data efficient!

Physics-informed neural networks modelling for systems with moving immersed boundaries: Application to an unsteady flow past a plunging foil

Rahul Sundar [a], Dipanjan Majumdar [a], Didier Lucor [b], Sunetra Sarkar [a,*]

[a] Department of Aerospace Engineering, Indian Institute of Technology Madras, Chennai, 600036, Tamil Nadu, India
[b] Université Paris-Saclay, CNRS, Laboratoire Interdisciplinaire des Sciences du Numérique (LISN), Orsay, F91405, France

Key outcomes and conclusions

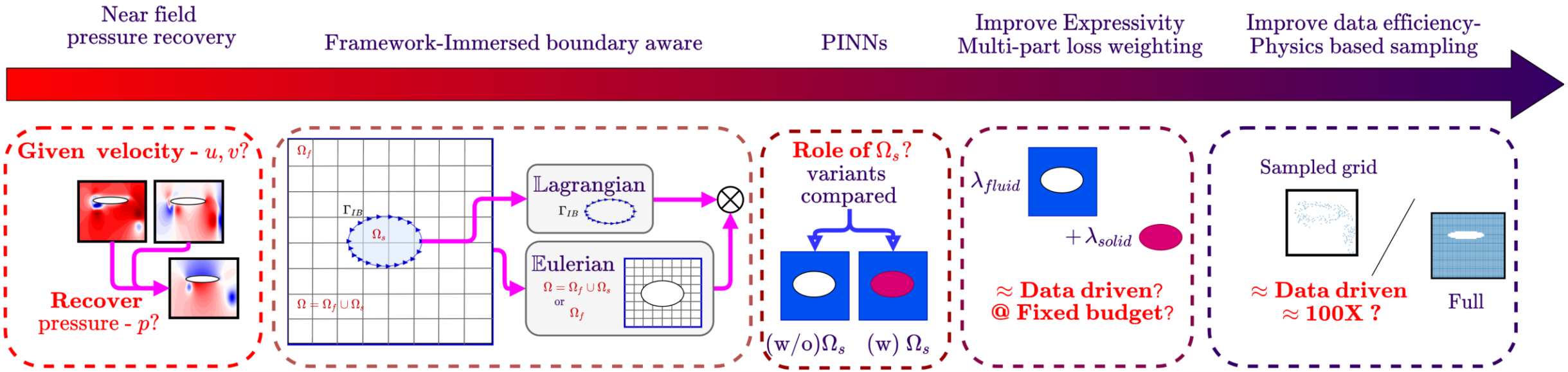

1. General framework!

2. Flexibly handled by PINNs!

3. λ_{fluid} - calibrated – to balance contributions from data & physics

4. Ω_s & L_{Phy}^{solid} not necessary if Γ_{IB} position and velocity known apriori.

5. If Γ_{IB} is unknown, MB-IBM-PINNs can be used for pressure recovery.

6. Physics based sampling - Data efficient!

Overview immersed boundary aware framework

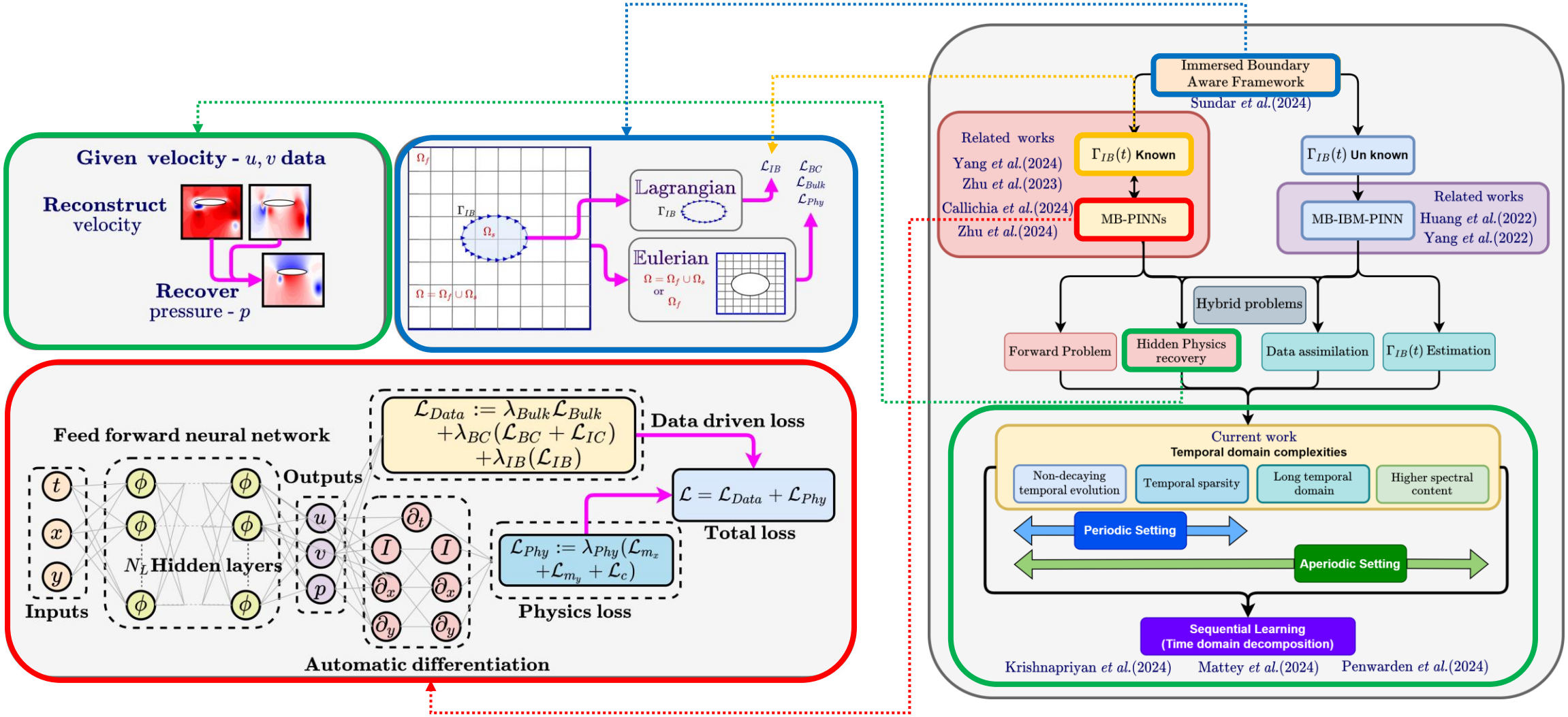

Velocity reconstruction

MB-FNN – Purely data-driven

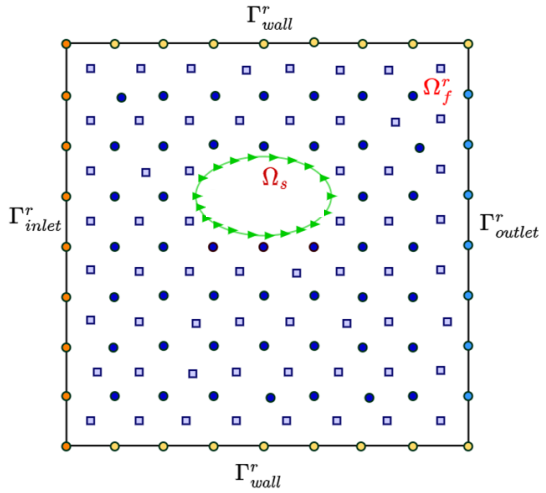

Hyper parameters: $N_L = 10, N_n = 100$, **ADAM** optimiser – N_{iter} **= 5e05** iterations, 3 training cycles – [1e-03, 5e-04, 1e-04], mini batch – 1.5e03

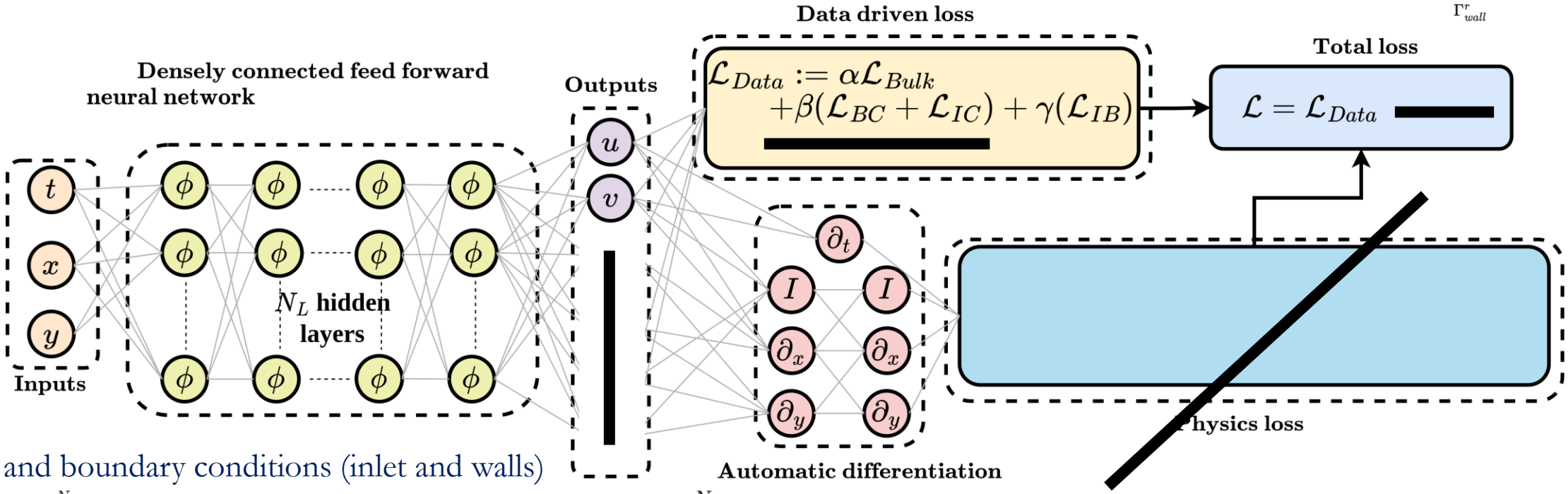

Initial and boundary conditions (inlet and walls)

$$\mathcal{L}_{IC} := \frac{1}{N_{IC}} \sum_{i=1}^{N_{IC}} \|\boldsymbol{u}(\boldsymbol{x}^i_{IC}, t_0) - \hat{\boldsymbol{u}}(\boldsymbol{x}^i_{IC}, t_0)\|^2_{L_2}$$

$$\mathcal{L}_{BC} := \frac{1}{N_k} \sum_{k=1}^{N_k} \left(\frac{1}{N_{BC_k}} \sum_{i=1}^{N_{BC_k}} \|\boldsymbol{u}(\boldsymbol{x}^i_{BC_k}, t^i) - \hat{\boldsymbol{u}}(\boldsymbol{x}^i_{BC_k}, t^i)\|^2_{L_2} \right)$$

$$\mathcal{L}_{IB} := \frac{1}{N_{IB}} \sum_{i=1}^{N_{IC}} \|\boldsymbol{u}(\boldsymbol{x}^i_{IB}, t_0) - \hat{\boldsymbol{u}}(\boldsymbol{x}^i_{IB}, t_0)\|^2_{L_2}$$ - No-slip velocity BC → Γ_{IB}: **Lagrangian** markers

$$\mathcal{L}_{Bulk} := \frac{1}{N_{Bulk}} \sum_{i=1}^{N_{Bulk}} \|\boldsymbol{u}(\boldsymbol{x}^i_{Bulk}, t^i) - \hat{\boldsymbol{u}}(\boldsymbol{x}^i_{Bulk}, t^i)\|^2_{L_2}$$ - Bulk velocity data reconstruction loss

Velocity reconstruction + pressure recovery

MB-PINN

[Raissi et al. (2019b) , Calicchia *et al.* (2023)]

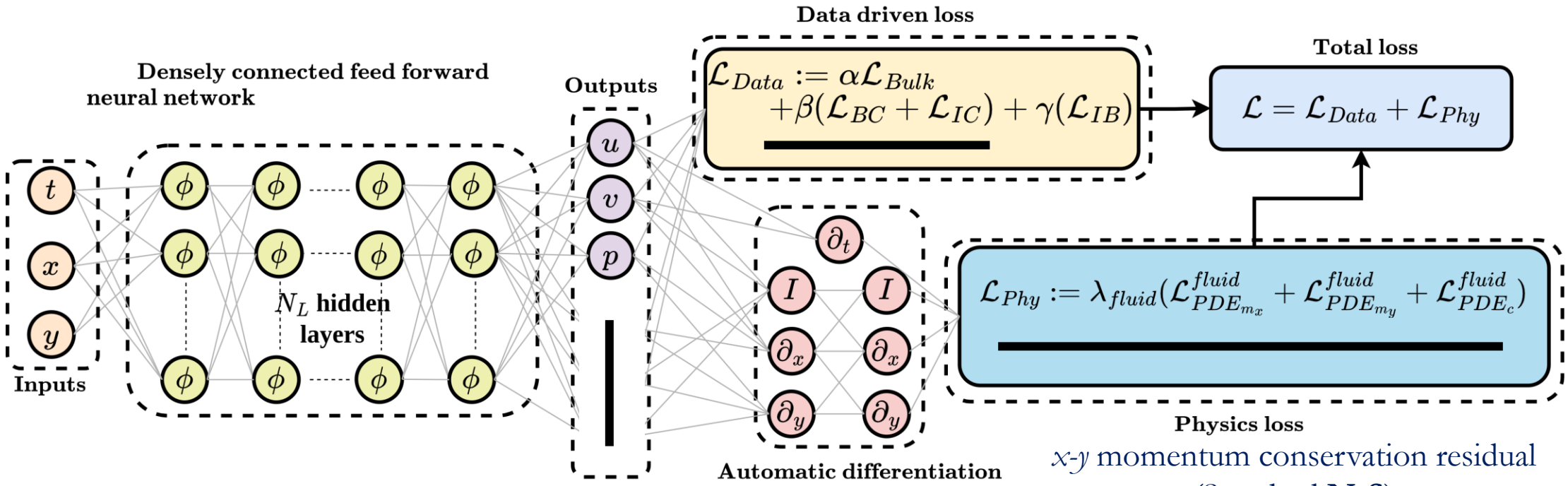

x-y momentum conservation residual (Standard **N-S**)

$$\mathcal{L}_{IB} := \frac{1}{N_{IB}} \sum_{i=1}^{N_{IC}} \|\boldsymbol{u}(\boldsymbol{x}^i_{IB}, t_0) - \hat{\boldsymbol{u}}(\boldsymbol{x}^i_{IB}, t_0)\|^2_{L_2}$$ - No-slip velocity BC → Γ_{IB}: **Lagrangian** markers

$$\mathcal{L}_{Bulk} := \frac{1}{N_{Bulk}} \sum_{i=1}^{N_{Bulk}} \|\boldsymbol{u}(\boldsymbol{x}^i_{Bulk}, t^i) - \hat{\boldsymbol{u}}(\boldsymbol{x}^i_{Bulk}, t^i)\|^2_{L_2}$$ - Bulk velocity data reconstruction loss

Velocity reconstruction + pressure recovery

MB-IBM-PINN

[IB-PINNs Huang et al. (2022)]

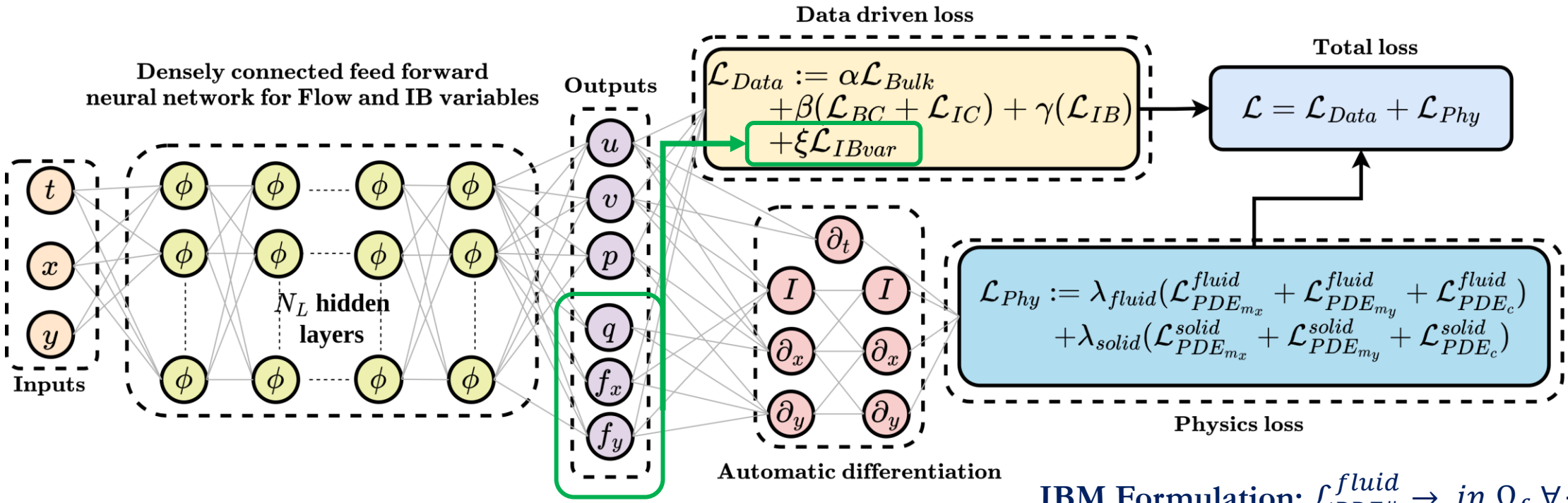

IBM auxillary variables constraint $\rightarrow \boldsymbol{f}, q \rightarrow 0 \; in \; \Omega_f \; \forall \; t/T$

$$\mathcal{L}_{IBvar} := \frac{1}{N_f} \sum_{i=1}^{N_{IBvar}} \left(\|f_x(\boldsymbol{x}^i_{IBvar}, t^i)\|^2_{L_2} + \|f_y(\boldsymbol{x}^i_{IBvar}, t^i)\|^2_{L_2} + \|q(\boldsymbol{x}^i_{IBvar}, t^i)\|^2_{L_2} \right)$$

IBM Formulation: $\mathcal{L}^{fluid}_{PDE\#} \rightarrow \; in \; \Omega_f \; \forall \frac{t}{T}$,
$\mathcal{L}^{solid}_{PDE\#} \rightarrow \; in \; \Omega_s \; \forall \frac{t}{T}$

Fluid-solid partitioned and weighted

Training and testing approach

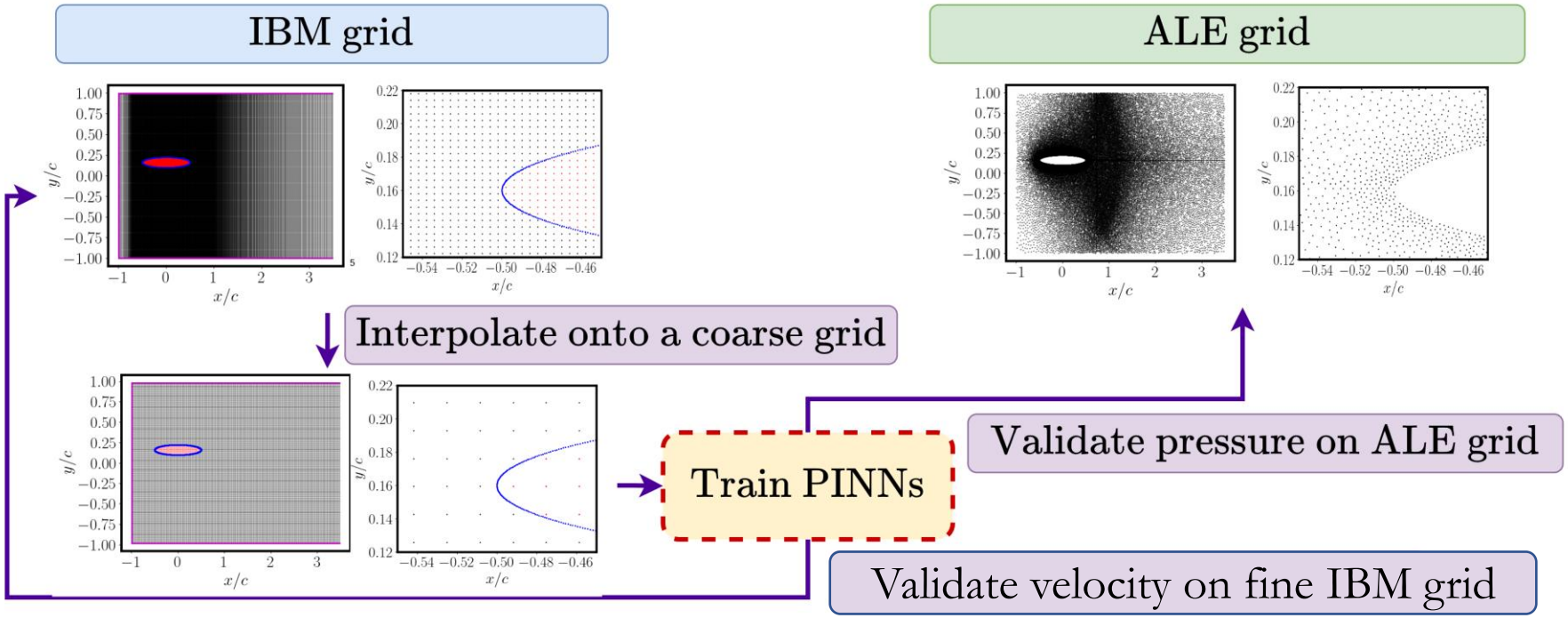

Table 1: Training and testing data sets used in the current study. Here, for each snapshot, the boundary points $N_{IB} = 1000$, $N_{wall} = 540$, $N_{inlet} = 120$ and $N_{IC} = 31500$. here, the ratio of data points in the coarse data set $\Theta_{Data} = 100 \times \frac{N_{Bulk}}{N_{Ref}}$ with $N_{Ref} = 651 \times 500 \times 81 = 2.63655e07$ points as in the Ref-IBM database.

Data set	N_x	N_y	N_t	$\Delta t/T$	$(Nx \times Ny \times Nt)$	N_{Bulk}	N_{res}^{fluid}	N_{res}^{solid}	Θ_{Data}
Ref-IBM	651	500	81	0.025	2.6365e07	-	-	-	-
Ref-ALE	-	-	81	0.025	4.05e06	-	-	-	-
CI	270	120	41	0.05	**1.3284e06**	1.2915e06	1.2915e06	1.476e04	4.8984%

Effect of fluid-solid partitioning/ weighting

Predictions at test time $t/T = 0.375$

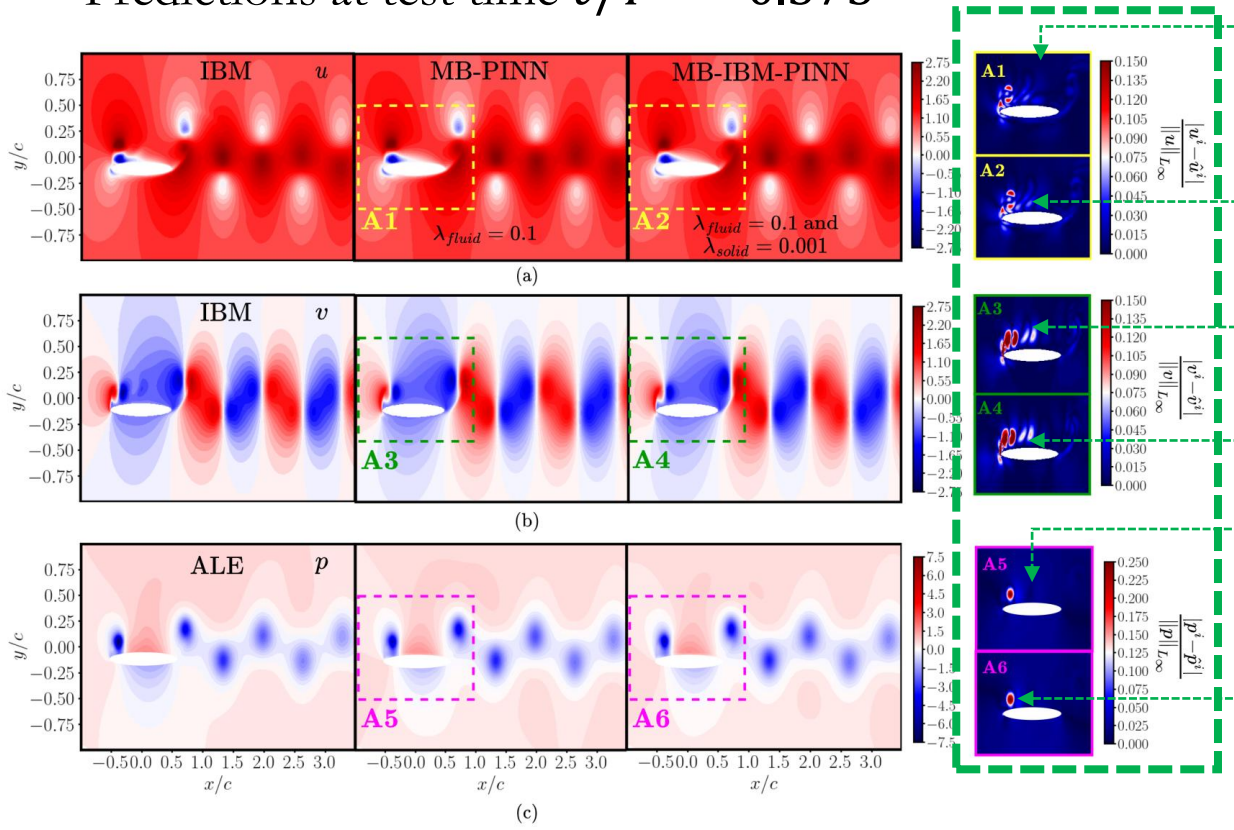

Errors localised & high around the LEV (**Z**)

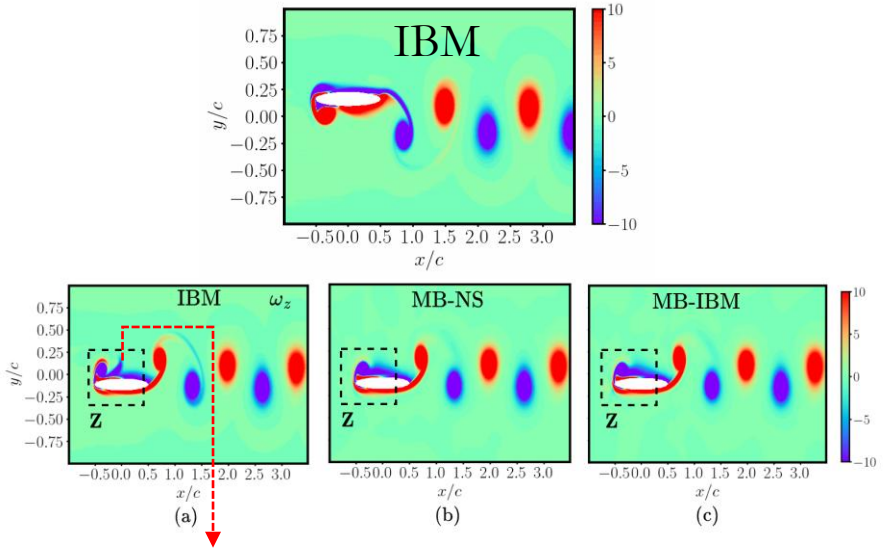

Secondary vortex structure not captured

Baseline MB-PINN ~ MB-IBM-PINN

$\lambda_{fluid} = 0.1, \lambda_{solid} = 0.001$

Further λ_{fluid} reduction - **Pressure field & vortex structures** improve?

$\lambda_{solid} \ll \lambda_{fluid}$ – **Role of solid region?**

Comparing optimal MB-PINN models

MB-PINN - B1 : $\lambda_{fluid} = 0.001, S_{\omega_z} = 100\%$

B2 : $\lambda_{fluid} = 0.01$ *and* $S_{\omega_z} = 5\%$

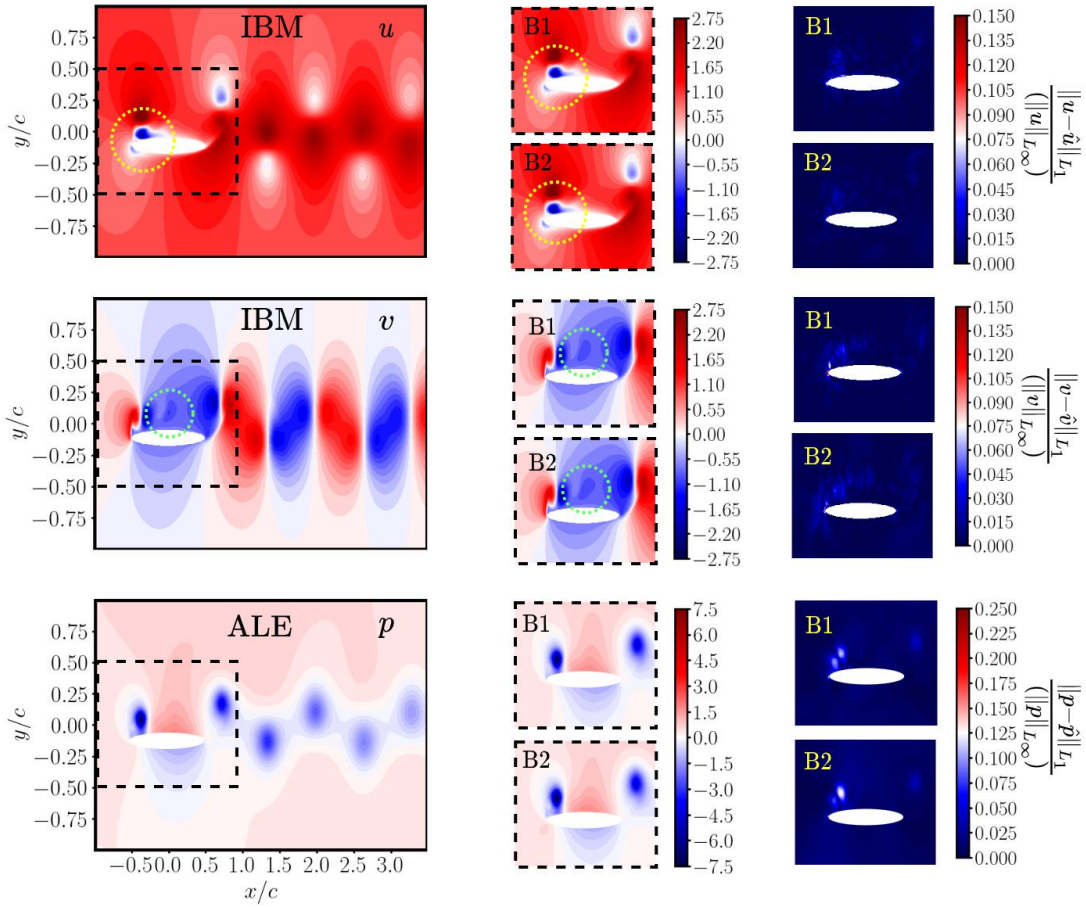

Purely data driven

Physics loss relaxation (A)

(A) + Physics based sampling

Model	Accuracy			
FNN	RMSE	MAE	R^2	rRMSE
u	5.8e-03	2.1e-03	9.999e-01	0.51
v	6.5e-03	2.3e-03	9.998e-01	1.31
	$\lambda_{fluid} = 0.1$ (Baseline)			
MB-PINN	RMSE	MAE	R^2	rRMSE
u	2.7e-02	1.1e-02	9.994e-01	2.41
v	3.0e-02	1.2e-02	9.961e-01	6.01
p	1.7e-01	1.0e-01	9.781e-01	13.41
	$\lambda_{fluid} = 0.001$			
MB-PINN	RMSE	MAE	R^2	rRMSE
u	9.6e-03	3.8e-03	9.999e-01	0.84
v	8.3e-03	3.3e-03	9.997e-01	1.67
p	8.9e-02	5.5e-01	9.943e-01	7.14
	$\lambda_{fluid} = 0.01$, $S_{\omega_z} = 5\%$			
MB-PINN	RMSE	MAE	R^2	rRMSE
u	8.6e-03	4.9e-03	9.999e-01	0.75
v	8.2e-03	4.7e-03	9.997e-01	1.64
p	9.1e-02	5.8e-02	9.938e-01	7.28

(In %)

Use Cases for periodic regime of unsteady flows past moving bodies

A: Simultaneous data reconstruction and hidden variable recovery

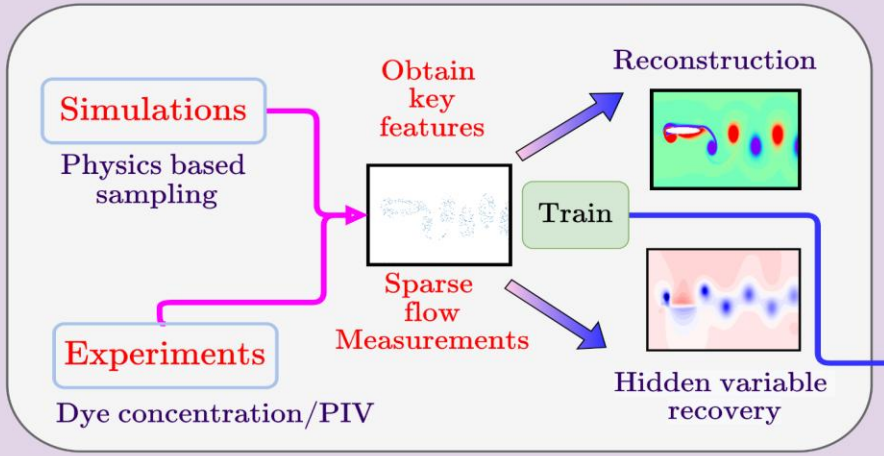

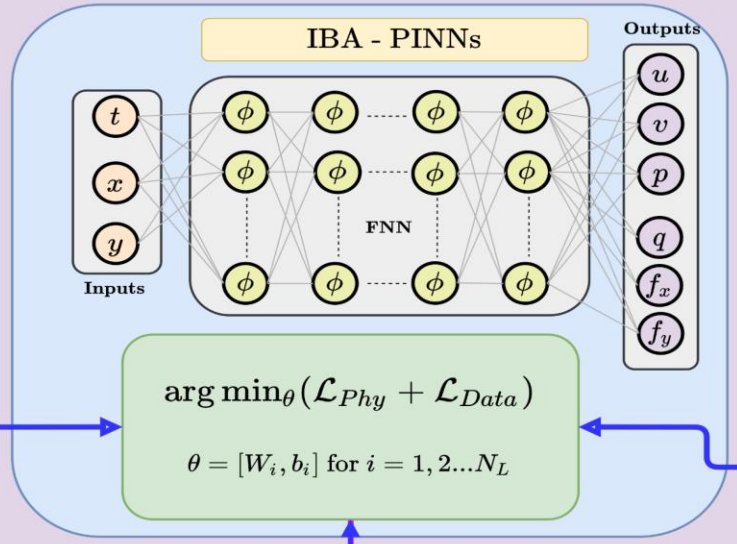

B: Query model in time

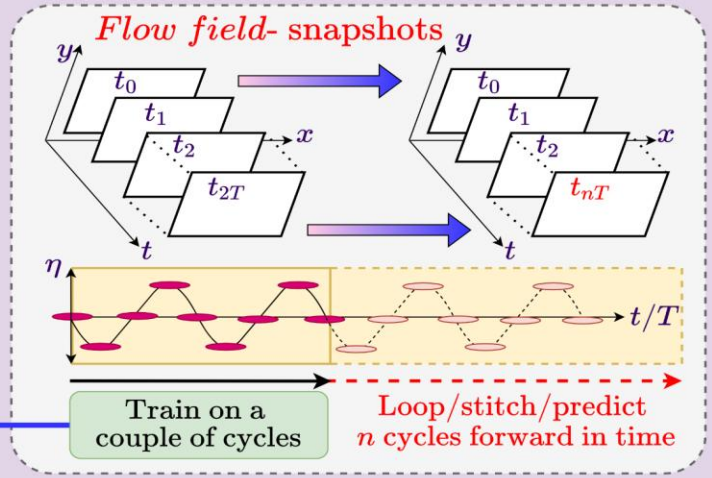

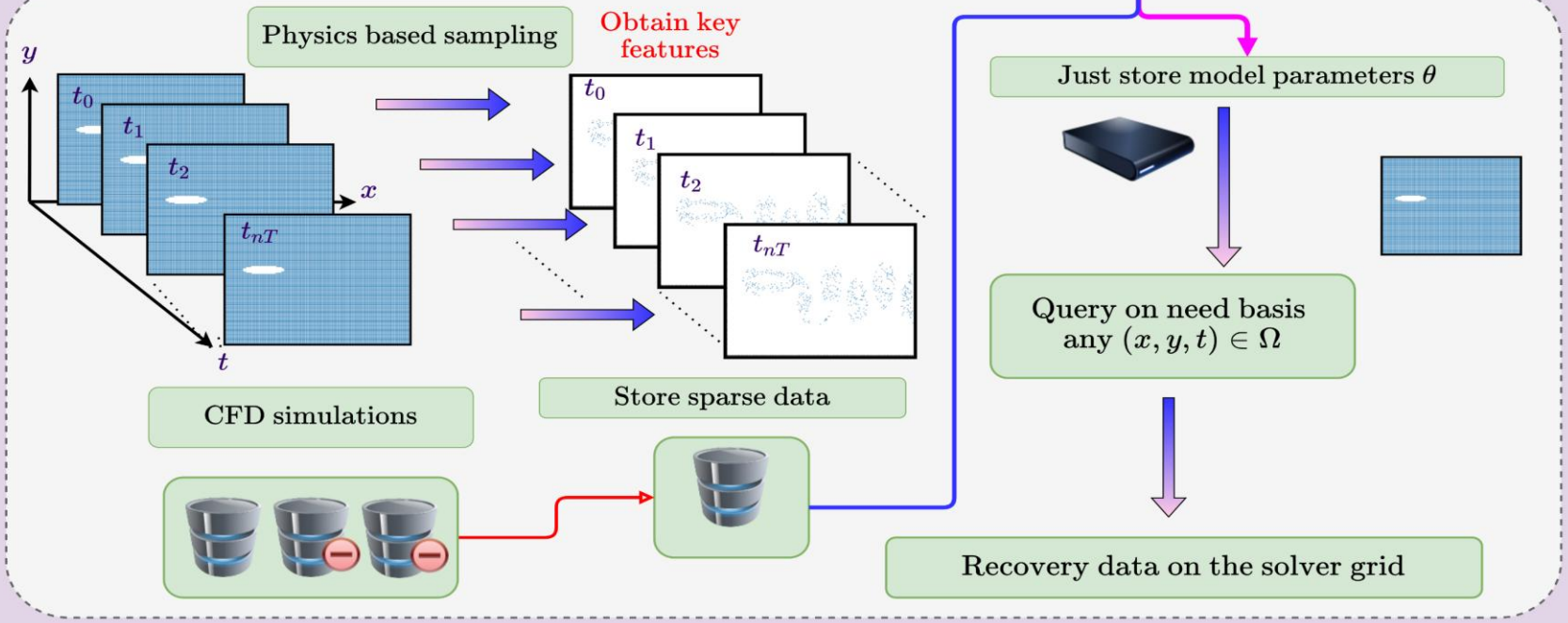

Other possibilities

D: Parametric surrogate and query models.
Solve complex optimisations problem

E: Transfer learn/fine-tune pre-trained models to model similar or more complex flows

Outcomes

Non-intrusive recovery

>100X Memory savings

C: Memory savings and space-time querying

Quasi-Periodic flow case study

Preferential sampling and relaxing of L_{IB} ($\lambda_{IB} = 1, 0.1, 0.01, 0.001$)

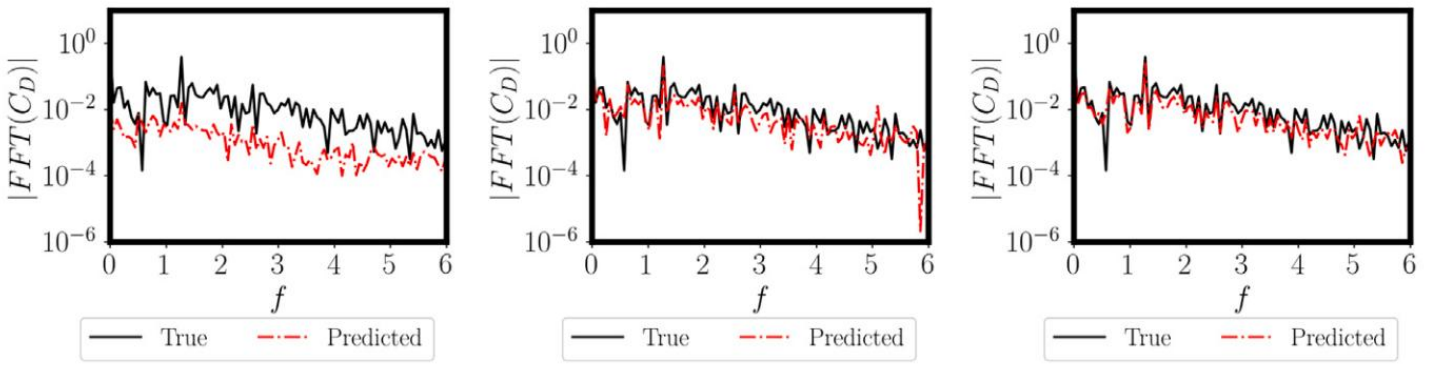

(a) $\mathbf{M0}, VS, \lambda_{IB} = 1, \Omega_1^r, n = 225$ (b) $\mathbf{M2}_{TD+TLLR}, PVS, \lambda_{IB} = 1, \Omega_2^r$ (c) $\mathbf{M2}_{TD+TLLR}, PVS, \lambda_{IB} = 0.001, \Omega_2^r$

- Preferential sampling + IB loss relaxation **improves temporal spectral recovery**
- CL-CD phase portraits **qualitatively capture the quasi-periodic dynamics.**
- **CD underpredicted** -> Due to **temporal sparsity** and **low data quality**

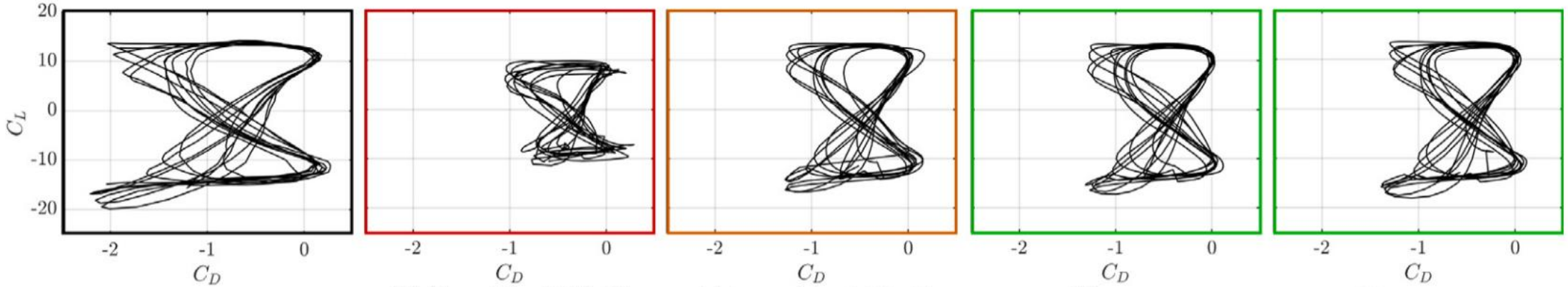

(a) IBM (b) $\Delta t_{Bulk}/T = 0.125, \Omega_1^r$ $\lambda_{IB} = 1$ (c) $\Delta t_{Bulk}/T = 0.125, \Omega_2^r$ $\lambda_{IB} = 0.001$ (d) $\Delta t_{Bulk}^{NF}/T = 0.125$ $\Delta t_{Bulk}^{FF}/T = 0.5, \Omega_2^r$ $\lambda_{IB} = 0.001$ (e) $\Delta t_{Bulk}^{NF}/T = 0.125, \Omega_3^r$ $\lambda_{IB} = 0.001$

PINNs for moving boundary problems

Authors (Year)	Problem considered	System(s) considered	Remarks/Contributions
Raissi *et al.* (1998)	Hidden physics recovery	VIV of a 2D cylinder	PINNs in body attached frame
Yang *et al.* (2021)	Forward solutions	Linear Elliptic and parabolic 2D PDEs with moving boundaries	Fictitious domain based PINNs (FDM-PINNs) proposed
Wang *et al.* (2020)	Forward and inverse system identification	Free boundary (Stefan) problems	Deep Stefan PINNs [Stacked PINNs]
Calicchia *et al.* (2023)	Pressure recovery from planar PIV velocity fields	Swimming fish	PINNs operating in fluid region alone
Huang *et al.* (2022)	Forward solution of IBM modified NS equations	2D Cylinder	IB-PINNs operating over the entire Eulerian grid.
Ours (2024, 2025)	**Pressure recovery from velocity data**	**2D Plunging foil**	**An Immersed boundary aware framework** proposed, **NS and IBM based PINN** formulations, **role of solid region explained**, **data-efficient physic- based sampling proposed**
Zhu *et al.* (2024)	Forward and inverse problems	2D and 3D single/multiple moving boundary unsteady flow examples	PINNs (equivalent to our MB-PINNs) were successful for inverse pressure recovery, forward (very short time-domain) problems.

Other research efforts at Bio-Mimetics and Dynamics Lab, IIT Madras

Bio-Mimetics & Dynamics Lαβ

Analysis

Understanding training of PINNs
Sundar et al. (2024)
Preprint: https://arxiv.org/pdf/2402.17346

Quantify input subdomain level contributions to the loss

$$\nabla_\theta \mathcal{L}_* = \left(\sum_{i=1}^{3} \left(p_{Zi} \nabla_\theta \mathcal{L}_*^{Zi} \right) \right)$$

Dimensionality reduction and modal analysis

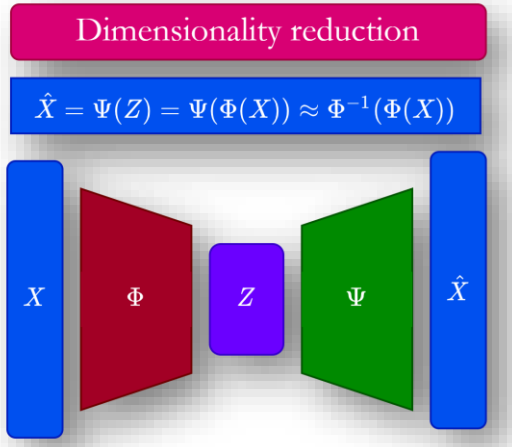

Comparative analysis of model reduction techniques for flapping wing dynamics
Arvind Thirunavukkarasu et al., *POF, (2024)*

Input subdomain level analysis

Rahul Sundar, Didier Lucor, and Sunetra Sarkar, Preprint available: https://arxiv.org/pdf/2402.17346

- An **input subdomain splitting of loss gradients and novel metrics were** proposed to quantify spatial imbalances in loss calculations.
- **Dominant spatial zone** is the **moving body region (Z1)** across test cases followed by the wake region (Z2) – due to relative strength of flow-field gradients in **Z1.**
- The analysis also served as a means to further **establish that vorticity cut off sampling in a way alleviates vanishing gradients problem.**

Perspectives:

- **Improved interpretability!** Can extend to **spatio-temporal-parametric input domains too!**
- Can enable design of **better training strategies.**

Post process - after model training

Or even in-situ while training

1. Visualize gradient distributions – (zonal and overall)

$$\nabla_\theta \mathcal{L}_* = \left(\sum_{i=1}^{3} \left(p_{Zi} \nabla_\theta \mathcal{L}_*^{Zi} \right) \right)$$

2. Quantify contributions through relative zonal gradient magnitude statistics

$$\mu_*^{Zi} = p_{Zi} \frac{\overline{|\nabla_\theta \mathcal{L}_*^{Zi}|}}{\overline{|\nabla_\theta \mathcal{L}_*|}}$$

$$\sigma_*^{Zi} = p_{Zi} \frac{\mathrm{std}\{|\nabla_\theta \mathcal{L}_*^{Zi}|\}}{\mathrm{std}\{|\nabla_\theta \mathcal{L}_*|\}}$$

References

1. Chin, Diana D., and David Lentink. "Flapping wing aerodynamics: from insects to vertebrates." *Journal of Experimental Biology* **219.7** (2016): 920-932.
2. Abdelkefi, Abdessattar. "Aeroelastic energy harvesting: A review." *International Journal of Engineering Science* **100** (2016): 112-135.
3. Bearman, P. W. "Circular cylinder wakes and vortex-induced vibrations." *Journal of Fluids and Structures* **27.5-6** (2011): 648-658.
4. I. E. Lagaris, A. Likas and D. I. Fotiadis, "Artificial neural networks for solving ordinary and partial differential equations," in *IEEE Transactions on Neural Networks*, vol. 9, no. 5, pp. 987-1000, Sept. 1998, doi: 10.1109/72.712178.
5. Fukami, K., Hasegawa, K., Nakamura, T. *et al.* Model Order Reduction with Neural Networks: Application to Laminar and Turbulent Flows. *SN COMPUT. SCI.* **2,** 467 (2021). https://doi.org/10.1007/s42979-021-00867-3
6. Majumdar, D. ,et. al, "Capturing the dynamical transitions in the flow-field of a flapping foil using Immersed Boundary Method." *Journal of Fluids and Structures* , **95** (2020): 102999.
7. Menon, K., & Mittal, R. (2020). Dynamic mode decomposition-based analysis of flow over a sinusoidally pitching airfoil. *Journal of Fluids and Structures*, **94**, 102886.
8. Balajewicz, M., & Farhat, C. (2014). Reduction of nonlinear embedded boundary models for problems with evolving interfaces. *Journal of Computational Physics*, *274*, 489-504.
9. Hornik, K., et.al "Multilayer feedforward networks are universal approximators." *Neural networks* **2.5** (1989): 359-366.
10. Sirovich, Lawrence. "Turbulence and the dynamics of coherent structures. I. Coherent structures." *Quarterly of applied mathematics,* **45.3** (1987): 561-571.
11. Baldi, Pierre, and Kurt Hornik. "Neural networks and principal component analysis: Learning from examples without local minima." *Neural networks,* **2.1** (1989): 53-58.

References

12. Kutz, J. Nathan. "Deep learning in fluid dynamics." *Journal of Fluid Mechanics* **814** (2017): 1-4.
13. Brunton, S. L.,et. al. "Machine learning for fluid mechanics." *Annual Review of Fluid Mechanics,* **52** (2020): 477-508.
14. Karniadakis, G. E., et al. "Physics-informed machine learning." *Nature Reviews Physics* 3.6 (2021): 422-440.
15. Benner, P., et.al. "A survey of projection-based model reduction methods for parametric dynamical systems." *SIAM review* **57.4** (2015): 483-531.
16. Yu, J., et. al. "Non-intrusive reduced-order modeling for fluid problems: A brief review." *Proceedings of the Institution of Mechanical Engineers, Part G: Journal of Aerospace Engineering* **233.16** (2019): 5896-5912.
17. Gupta, R., & Jaiman, R. (2022). A hybrid partitioned deep learning methodology for moving interface and fluid–structure interaction. *Computers & Fluids*, *233*, 105239.
18. Farhat, C., et al. "5 Computational bottlenecks for PROMs: precomputation and hyperreduction." *Snapshot-Based Methods and Algorithms*. De Gruyter, 2020. 181-244.
19. Lee, K., and Kevin T. C. "Model reduction of dynamical systems on nonlinear manifolds using deep convolutional autoencoders." *Journal of Computational Physics* 404 (2020): 108973.
20. Schmid, Peter J. "Dynamic mode decomposition of numerical and experimental data." *Journal of fluid mechanics* 656 (2010): 5-28.
21. Gao, H., et. al "Non-intrusive model reduction of large-scale, nonlinear dynamical systems using deep learning." *Physica D: Nonlinear Phenomena,* **412** (2020): 132614.
22. Gao, H., & Wei, M. (2014). Global model reduction for flows with moving boundary. In *52nd aerospace sciences meeting* (p. 0222).
23. Eivazi, H., et al. "Deep neural networks for nonlinear model order reduction of unsteady flows." *Physics of Fluids* ,**32.10** (2020): 105104.
24. Calicchia, Michael A., et al. "Reconstructing the pressure field around swimming fish using a physics-informed neural network." *Journal of Experimental Biology 226.8 (2023): jeb244983*.
25. Zhu, Yongzheng, et al. "Physics-informed neural networks for incompressible flows with moving boundaries." *Physics of Fluids* 36.1 (2024).

Velocity reconstruction + pressure recovery

MB-PINN

[Raissi et al. (2019b) , Calicchia *et al.* (2023)]

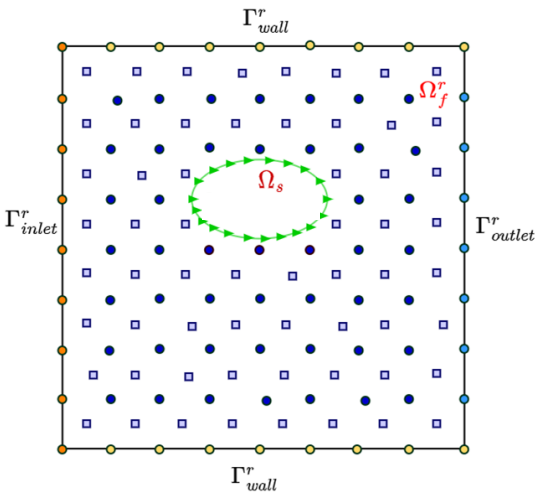

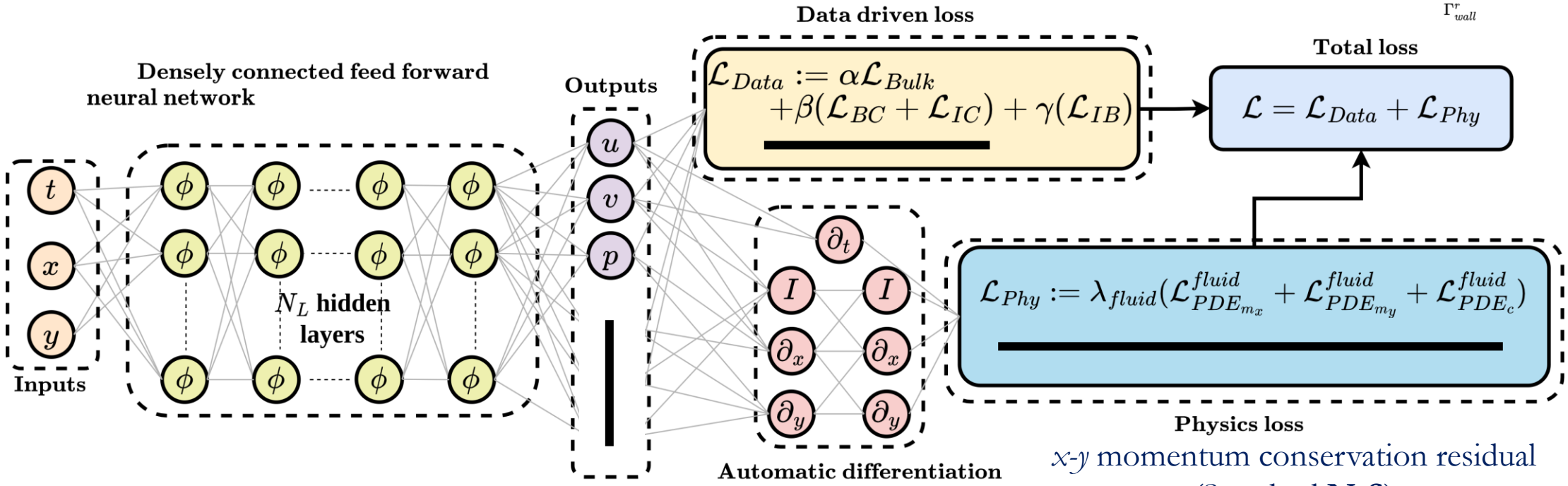

x-y momentum conservation residual (Standard **N-S**)

$$\mathcal{L}_{IB} := \frac{1}{N_{IB}} \sum_{i=1}^{N_{IC}} \|\boldsymbol{u}(\boldsymbol{x}^i_{IB}, t_0) - \hat{\boldsymbol{u}}(\boldsymbol{x}^i_{IB}, t_0)\|^2_{L_2}$$ - No-slip velocity BC → Γ_{IB}: **Lagrangian** markers

$$\mathcal{L}_{Bulk} := \frac{1}{N_{Bulk}} \sum_{i=1}^{N_{Bulk}} \|\boldsymbol{u}(\boldsymbol{x}^i_{Bulk}, t^i) - \hat{\boldsymbol{u}}(\boldsymbol{x}^i_{Bulk}, t^i)\|^2_{L_2}$$ - Bulk velocity data reconstruction loss

Velocity reconstruction + pressure recovery

MB-IBM-PINN

[IB-PINNs Huang et al. (2022)]

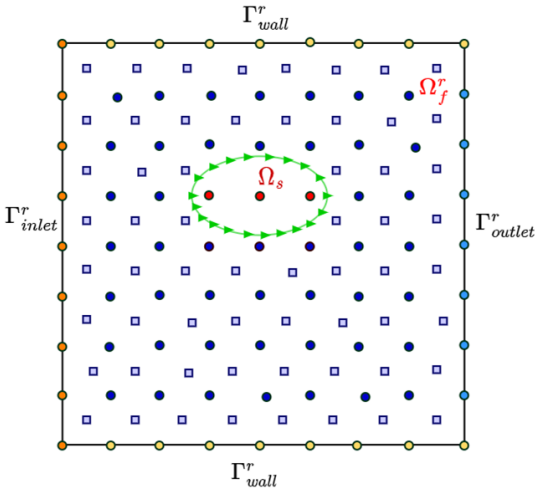

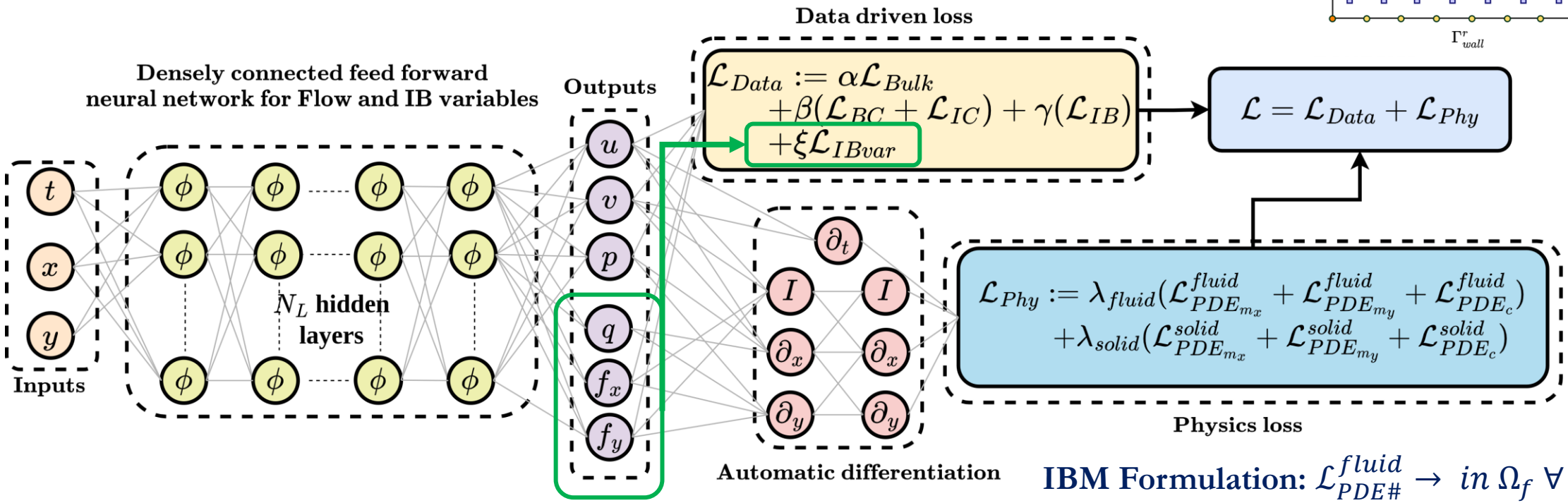

IBM auxillary variables constraint → $\boldsymbol{f}, q \to 0\ in\ \Omega_f\ \forall\ t/T$

$$\mathcal{L}_{IBvar} := \frac{1}{N_f}\sum_{i=1}^{N_{IBvar}} \left(\|f_x(\boldsymbol{x}^i_{IBvar}, t^i)\|^2_{L_2} + \|f_y(\boldsymbol{x}^i_{IBvar}, t^i)\|^2_{L_2} + \|q(\boldsymbol{x}^i_{IBvar}, t^i)\|^2_{L_2}\right)$$

IBM Formulation: $\mathcal{L}^{fluid}_{PDE\#} \to in\ \Omega_f\ \forall \frac{t}{T}$,

$\mathcal{L}^{solid}_{PDE\#} \to in\ \Omega_s\ \forall \frac{t}{T}$

Fluid-solid partitioned and weighted